

This discussion paper is/has been under review for the journal Atmospheric Chemistry and Physics (ACP). Please refer to the corresponding final paper in ACP if available.

Distributions and radiative forcings of various cloud types based on active and passive satellite datasets – Part 1: Geographical distributions and overlap of cloud types

J. Li¹, J. Huang¹, K. Stamnes², T. Wang¹, Y. Yi³, X. Ding¹, Q. Lv¹, and H. Jin¹

¹Key Laboratory for Semi-Arid Climate Change of the Ministry of Education, College of Atmospheric Sciences, Lanzhou University, Lanzhou, China

²Department of Physics and Engineering Physics, Stevens Institute of Technology, Hoboken, NJ, USA

³Key Laboratory of Western China's Environmental Systems (Ministry of Education), Collaborative Innovation Centre for Arid Environments and Climate Change, Lanzhou University, Lanzhou 73000, China

Title Page

Abstract

Introduction

Conclusions

References

Tables

Figures

◀

▶

◀

▶

Back

Close

Full Screen / Esc

Printer-friendly Version

Interactive Discussion



Received: 12 February 2014 – Accepted: 4 April 2014 – Published: 25 April 2014

Correspondence to: J. Huang (hjp@lzu.edu.cn)

Published by Copernicus Publications on behalf of the European Geosciences Union.

ACPD

14, 10463–10514, 2014

Distributions and
overlap of various
cloud types

J. Li et al.

Title Page

Abstract

Introduction

Conclusions

References

Tables

Figures

|◀

▶|

◀

▶

Back

Close

Full Screen / Esc

Printer-friendly Version

Interactive Discussion



Abstract

Based on four year' 2B-CLDCLASS-Lidar (Radar-Lidar) cloud classification product from CloudSat, we analyze the geographical distributions of different cloud types and their co-occurrence frequency across different seasons, moreover, utilize the vertical distributions of cloud type to further evaluate the cloud overlap assumptions.

The statistical results show that more high clouds, altocumulus, stratocumulus or stratus and cumulus are identified in the Radar-Lidar cloud classification product compared to previous results from Radar-only cloud classification (2B-CLDCLASS product from CloudSat). In particularly, high clouds and cumulus cloud fractions increased by factors 2.5 and 4–7, respectively. The new results are in more reasonable agreement with other datasets (typically the International Satellite Cloud Climatology Project (ISCCP) and surface observer reports). Among the cloud types, altostratus and altocumulus are more popular over the arid/semi-arid land areas of the Northern and Southern Hemispheres, respectively. These features weren't observed by using the ISCCP D1 dataset.

For co-occurrence of cloud types, high cloud, altostratus, altocumulus and cumulus are much more likely to co-exist with other cloud types. However, stratus/stratocumulus, nimbostratus and convective clouds are much more likely to exhibit individual features. After considering the co-occurrence of cloud types, the cloud fraction based on the random overlap assumption is underestimated over the vast ocean except in the west-central Pacific Ocean warm pool. Obvious overestimations are mainly occurring over land areas in the tropics and subtropics. The investigation therefore indicates that incorporate co-occurrence information of cloud types based on Radar-Lidar cloud classification into the overlap assumption schemes used in the current GCMs possible be able to provide an better predictions for vertically projected total cloud fraction.

ACPD

14, 10463–10514, 2014

Distributions and overlap of various cloud types

J. Li et al.

Title Page	
Abstract	Introduction
Conclusions	References
Tables	Figures
◀	▶
◀	▶
Back	Close
Full Screen / Esc	
Printer-friendly Version	
Interactive Discussion	



1 Introduction

As the most important regulators of the Earth's climate system, clouds may significantly affect the radiation budget, the hydrological cycle and the large-scale circulation of the Earth (Hartmann et al., 1992; Stephens, 2005). However, due to an incomplete knowledge of the underlying physical processes, clouds are still poorly represented in climate and weather models (Zhang et al., 2005), and thus are considered as the major source of uncertainty in predictions of climate change by general circulation models (GCMs) (Cess et al., 1990).

In various cloud properties, cloud type and their overlap, which are two of the important cloud macro-physical properties, are of particular significance for the earth's radiation budget and hydrological cycle. On the one hand, different cloud types are governed by different kinds of atmospheric motions and have different microphysical properties, thus can result in quite different cloud radiative forcings (Ackerman et al., 1988; Betts and Boers, 1990; Hartmann et al., 1992) and may bring about distinguishing precipitation forms and intensities. On the other hand, frequent co-occurrences of different cloud types in the atmosphere further intensify the complexity of present cloud climatology studies. Cloud overlap variations can significantly change atmospheric radiative heating/cooling rates, atmospheric temperature, hydrological processes, and daily variability (Chen and Cotton, 1987; Liang and Wu, 2005; Morcrette and Jakob, 2000), with important implications for the radiative balance of the surface-troposphere system (Stephens et al., 2004). In addition, the presence of cloud overlap also introduces significant errors in the retrievals of cloud properties with passive satellite cloud retrieval techniques (Stephens et al., 2004), which are based on the typical single-layered cloud assumption. Therefore, to further aid radiation calculations of climate prediction models and help understand cloud physical processes and evaluate the schemes for generating clouds in those models, it is necessary to know not only the amount and distribution of each cloud type but also a detailed description of the co-occurrence of different cloud types (Warren et al., 1985).

Title Page	
Abstract	Introduction
Conclusions	References
Tables	Figures
	
	
Back	Close
Full Screen / Esc	
Printer-friendly Version	
Interactive Discussion	



Distributions and overlap of various cloud types

J. Li et al.

Title Page

Abstract

Introduction

Conclusions

References

Tables

Figures

◀

▶

◀

▶

Back

Close

Full Screen / Esc

Printer-friendly Version

Interactive Discussion



Until now, many related works with cloud type and cloud overlap, which based on several fundamentally different types of passive observational datasets (typically the International Satellite Cloud Climatology Project (ISCCP) and surface observer reports), have focused on the geographic distributions and long-term variations of different cloud types (e.g. Rossow and Schiffer, 1991, 1999; Hahn et al., 2001; Warren et al., 2007; Eastman et al., 2011, 2013), and their radiative effect investigations (Hartmann et al., 1992; Chen et al., 2000; Yu et al., 2004), or specially aimed at the cloud properties retrieval of multilayered cloud by using multi-channel measurements from passive sensors (Chang and Li, 2005a, b; Huang et al., 2005, 2006a; Minnis et al., 2007), and the statistics of cloud overlap based on the surface weather reports and the measurements from the ground-based cloud radar (Warren et al., 1985; Minnis et al., 2005; Hogan and Illingworth, 2000). However, these studies have non-negligible limitations and uncertainties due to passive detection methods and cloud classification algorithms generally fail to effectively detect multilayered clouds. First, the existence of overlapping cloud layers may cause the upper clouds to be hidden from the view of a ground observer, and lower clouds to be hidden from the view of a passive satellite which leads to a significant underestimation of high and low cloud frequencies by surface observer reports and ISCCP, thus introduce significant biases in the trends analysis of cloud-type cover, retrievals of cloud properties and evaluation of cloud radiative forcings of different cloud types. Second, most of these studies are limited to specific locations, time periods or multilayered cloud systems, systematic researches about the co-occurrence statistics of different cloud types on a global scale still have received much less attention. Thus, compared to passive observations, observational studies of cloud types and co-occurrence variations on a global scale based on active remote sensing from satellites are recognized as an important step to improve cloud representation in weather and climate models, and promote the development of global cloud climatology studies.

The launch of the millimeter wavelength cloud profiling radar (CPR) on CloudSat (Stephens et al., 2002) and the cloud-aerosol lidar with orthogonal polarization (CALIOP) (Winker et al., 2007) on CALIPSO in late April 2006 provide us an unprece-

Distributions and overlap of various cloud types

J. Li et al.

Title Page

Abstract

Introduction

Conclusions

References

Tables

Figures

◀

▶

◀

▶

Back

Close

Full Screen / Esc

Printer-friendly Version

Interactive Discussion



dented opportunity for detailed studying the three-dimensional structures of cloud and related radiative forcings on a global scale. Since becoming available in the middle of June 2006, CALIPSO and CloudSat data have been widely used to investigate the three-dimensional distributions and structures of hydrometeor, and improve the cloud overlap assumption used in GCMs (e.g. Luo et al., 2009; Kato et al., 2010; Barker, 2008). In this study, we plan to use the latest cloud classification product based on the combined measurements of these two active sensors to investigate the geographical distributions and co-occurrence frequencies of different cloud types, and further evaluate how well the cloud overlap assumptions can characterize the overlap of two apparently separated cloud types. Although some statistical results are in reasonable agreement with previous works, additional new insights are also gained in this investigation. It is hoped that these new results will be useful for future GCM evaluation and improvement.

The study is organized as follows. The dataset used is described in Sect. 2. Section 3 mainly analyzes the global, zonal distributions and diurnal variations of different cloud types based on the new dataset. Comparisons of global mean fractions of different cloud types from several datasets are provided in Sect. 4. Section 5 firstly gives the zonal distributions and global statistics of co-occurrence frequency of different cloud types, then further evaluates the performance of cloud overlap assumptions based on co-occurrence frequency of cloud types.

2 Data

In the following study, four years (2007–2010) of data from the latest release of the CloudSat 2B-CLDCLASS-Lidar (version 1.0) product, which is referred as Radar-Lidar cloud classification, are collected to analyze cloud types and discuss their geographical distributions and overlap variations on a global scale. The algorithm of this product mainly is based on the study of Wang and Sassen (2001), which classified cloud types by combining the ranging capabilities of active sensors (Radar and Lidar) and the aux-

Distributions and overlap of various cloud types

J. Li et al.

Title Page

Abstract

Introduction

Conclusions

References

Tables

Figures

◀

▶

◀

▶

Back

Close

Full Screen / Esc

Printer-friendly Version

Interactive Discussion



type includes cirrus, cirrocumulus and cirrostratus, and the Cu cloud type represents cumulus congestus and fair weather cumulus. These types may be further classified into sub-types to refine ice water path (IWC) and liquid water path (LWC) retrievals. Followed the study of Sassen and Wang (2008), we also combine two level cloud types (St and Sc) as St + Sc in present study in order to compare the results with other datasets. Due to combine the unique complementary capabilities of Cloud profile radar (CPR) from CloudSat and space-based polarization lidar (CALIOP), some CPR weaknesses (e.g. high surface contamination in the lowest three to four vertical bins of CPR, and lower sensitivity to optically thin clouds) will be minimized in the latest Radar-Lidar cloud classification product, this eventually led to the significant improvement for High (cirrus or cirrostratus) and lower cloud types (such as, St, Sc and Cu) identification in the 2B-CLDCLASS-Lidar product (please see Table 1 about the detail information).

Following cloud parameters in the 2B-CLDCLASS-Lidar product are used in this study: cloud layer (CL), Cloud Layer Type (CLTY). In order to map the regional variability of the studied variable, we group the global area into $2^\circ \times 2^\circ$ grid boxes in order to collect a sufficient number of samples in each grid box. Following the definitions of cloud fraction and cloud amount by Hagihara et al. (2010), cloud-type fractions in the following study are defined as the ratio of the number of profiles for a certain cloud type to the total number of sample profiles within a given grid box during spring (March, April and May), summer (June, July and August), autumn (September, October and November) and winter (December, January and February). The cloud-type amounts in a given grid box are defined as the number of a certain cloud type profiles divided by the number of total cloud profiles collected in this box. In addition, cloud fraction differences for single-layered clouds and multilayered clouds (two or more cloud layers in a profile) between day- and night-time also are further analyzed and discussed in the investigation. It is worth noting that the full diurnal cycle cannot be captured by CALIPSO and CloudSat. Thus, the diurnal variations of cloud fraction or amount are referred as the cloud property differences between the two overpass times of these satellites. In addition, it needs further explanation is that combined space-based lidar in

Title Page	
Abstract	Introduction
Conclusions	References
Tables	Figures
◀	▶
◀	▶
Back	Close
Full Screen / Esc	
Printer-friendly Version	
Interactive Discussion	



Distributions and
overlap of various
cloud types

J. Li et al.

Title Page

Abstract

Introduction

Conclusions

References

Tables

Figures

◀

▶

Back

Close

Full Screen / Esc

Printer-friendly Version

Interactive Discussion



this 2B-CLDCLASS-Lidar product is used to improve the classifications of optically thin clouds and lower cloud types. Due to the strong solar noise signature, the difference of cloud types between day and night in present study will be affected by the solar noise effects, especially for cirrus of High cloud type. However, by analyzing the day-night difference of highest (and presumably optically thinnest) cirrus at the tropical tropopause, Sassen et al. (2008) showed that this type cirrus is not significantly different between day and night, but the frequency of deep convective anvil-cirrus somewhat below is noticeably greater at night. The observed diurnal variations of cirrus mostly reflect real cloud process (Sassen et al., 2009). For other cloud types, the uncertainty caused by the daylight noise for Lidar may be smaller. Thus, although slight overestimation is exist for the day-night difference of cirrus, the observed diurnal variations of different cloud types in this investigation still are reliable.

3 Geographical distributions and diurnal variations of different cloud types

3.1 Global distribution and diurnal variation of each cloud type

Figures 1 and 2 show the seasonal variations of mean day plus night frequencies and global distributions of the annual mean night minus day frequencies for different cloud types, averaged over $2^\circ \times 2^\circ$ grid boxes based on the 2B-CLDCLASS-Lidar product, respectively. In Fig. 1, from left to right, the columns present the cloud fractions of different cloud types during spring, summer, autumn and winter. As indicated by Fig. 1, the seasonal variations of spatial patterns and cloud fractions for most of the cloud types are obvious. High clouds (cirrus, cirrostratus and cirrocumulus) are (Fig. 1a1–d1) mainly concentrated in the inter-tropical convergence zone (ITCZ), which is correlated with deep convective clouds (see Fig. 1a7–d7) (Mace et al., 2006; Sassen et al., 2009), and the cloud fractions may exceed 60 % over the several typical high-value centers, such as the equatorial central South America, western Africa, Indonesia and the west-central Pacific Ocean warm pool. Due to the descending motions in the Hadley cell

Distributions and overlap of various cloud types

J. Li et al.

Title Page

Abstract

Introduction

Conclusions

References

Tables

Figures

◀

▶

◀

▶

Back

Close

Full Screen / Esc

Printer-friendly Version

Interactive Discussion



circulation, the small high cloud frequency is very apparent in the subtropics. It is worth noting that tropical high cloud fractions, especially at the several high-value centers, have noticeably higher frequencies at night compared to day (even exceeding 13.5 %) even if their patterns are quite similar, whereas high cloud frequencies in other regions (such as mid- to high latitudes) generally show small differences (see Fig. 2a1). For cirrus of high clouds, Sassen et al. (2008) found a global average frequency of cirrus cloud occurrence of 16.7 % (mean day plus night), with 15.2 % for day and 18.3 % for night based on A-train overpasses. In this study, the global average high cloud frequencies are 24.3 % and 29.3 % for day- and night-time, respectively. Therefore, it is clear that the corresponding globally averaged frequencies of cirrostratus and cirrocumulus are about 9.1 % and 11 % for day- and night-time, respectively. Although cirrus and cirrostratus/cirrocumulus both contribute to the diurnal variability of the total day-night difference of the high cloud fraction, the pattern of difference due to cirrus still is very close to that due to high clouds, and its difference accounts for a significant great proportion (about 62 %) of the globally averaged difference. In view of the high and thin tropopause transitional layer (TTL), cirrus clouds do not display a noticeable diurnal variation. Thus, the effect of CALIOP signal noise from scattered sunlight only can cause a small part of the total cirrus cloud occurrence differences (Sassen et al., 2008). The diurnal cirrus patterns mostly still reflect real cloud processes. The apparent day-night difference over the tropical ocean (such as, western coastline of continents) and tropical landmasses and island chains (such as, northern South America, equatorial Africa, and the western Pacific) are mainly caused by the prevalent subvisual (optical depth < 0.03) and thin cirrus clouds ($0.03 < \text{optical depth} < 0.3$), respectively (Sassen et al., 2009). However, the recent work by Behrangi et al. (2012) showed by using 2B-CLDCLASS product that high clouds are much more abundant during daytime over the ocean. The opposite diurnal variations between our analysis and their results thus are mainly due to the weak CPR sensitivity to cirrus clouds resulting in a lot of missing cirrus in their study, especially for subvisual cirrus. At other latitudes (such as mid- and high latitudes), cirrus may be formed by the different seasonal cirrus cloud generat-

Distributions and
overlap of various
cloud types

J. Li et al.

Title Page

Abstract

Introduction

Conclusions

References

Tables

Figures

◀

▶

◀

▶

Back

Close

Full Screen / Esc

Printer-friendly Version

Interactive Discussion



ing mechanisms, including deep convection, synoptic jet stream, orographic lifting and frontal activity (Sassen, 2002; Warren et al., 1985) or condensation trails from aircraft (Boucher, 1999; Minnis et al., 2004). Thus night/day differences at these latitudes also reflect diurnal differences of generating mechanisms.

As one of the mid-level cloud types, altostratus (Fig. 1a2–d2) is widely distributed at middle and high latitudes, such as over storm tracks and Antarctica. The obvious high-value centers are located at the Tibetan Plateau of China, northwest of USA and Canada and in most regions of Antarctica. But, they vary considerably across different seasons. For example, the altostratus cloud coverage over the Tibetan Plateau both during winter and spring reach maximum values (exceed 40 %), then apparently decrease in summer and autumn. Based on the ISCCP dataset, Yu et al. (2004) pointed out that the seasonal variations of nimbostratus and altostratus clouds over subtropical East Asia might be caused by the seasonal frictional and blocking effects of the Tibetan Plateau. In addition, during summer and autumn, the altostratus clouds also exhibit apparent high fractions (reaching 36 %) over Antarctica. Altostratus occurring at the mid- and high latitudes, are possibly related to the frequent frontal activities in these regions. For the day-night difference of altostratus (Fig. 2a2), more altostratus clouds can be seen over the south-polar region and central Africa during night compared to day. However, the pattern is opposite at other latitudes (such as, storm tracks).

Altocumulus (Ac) clouds (Fig. 1a3–d3) show a high occurrence frequency over land in tropical and subtropical regions, which are strongly correlated with deep convective activities (see Fig. 1a7–d7). The obvious seasonal variation of peak-value centers over land corresponds to the seasonal shift of ITCZ. In addition, altocumulus clouds over the India, Bangladesh (Subrahmanyam and Kumar, 2013), the southeast part of China, and the northern part of Australia also have high cloud fractions. The apparent diurnal variations of altocumulus mainly occur in the tropics (negative difference) and the polar regions (positive difference).

Figure 1a4–d4 demonstrate the seasonal distributions of strati-form clouds globally (that is, stratus and stratocumulus). Several significant and consistent high-value cen-

ters can be found over the semi-permanent subtropical marine stratocumulus sheets (Wood, 2012), such as the west coasts of North America, South America, and West Africa, where strati-form cloud fractions even may exceed 60 %. In addition, strati-form clouds also are widespread over the vast oceans of the Southern Hemisphere (cloud fraction beyond 50 %), particularly in the storm track where the super-cooled water clouds are very frequent as well (Hu et al., 2010). The larger stratocumulus cover for the Southern Hemisphere compared to the Northern Hemisphere may be driven by increased stability and subsidence related to the configuration of elevated terrain to their east (Xu et al., 2004). In addition, the noticeably higher frequencies of strati-form at night compared to day are found in our study. The results are consistent with other previous studies (Rozendaal et al., 1995; Bergman and Salby, 1996), and maybe mainly caused by the strong diurnal cycle of solar insolation and consequently radiative absorption of solar radiation during daytime in the upper levels of the cloud and large-scale dynamics (Wood et al., 2009). As indicated in Fig. 2a4, there are more strati-form clouds (even reaching 20 %) during nighttime distributed over the ocean of several subtropical stratocumulus regions. However, the pattern is inverse over land, especially over central Africa and equatorial central South America, where the strati-form cloud fraction difference between night and day can exceed 10 %.

Due to being driven by convective heating from below, cumulus clouds are mainly concentrated over the ocean between 30° S and 30° N (see Fig. 1a5–d5). Moreover, they are also observed much more frequently over ocean than over land, such as, the western and central tropical and subtropical oceans (Norris, 1998), which is probably due to the proximity to a water source. The high values and broad maximum of observed cumulus frequency in equatorial and subtropical latitudes over oceans of both hemispheres represent the persistent occurrence of “trade cumulus” in these regions (Warren et al., 1985). Its peak values may exceed 20 % over the tropical ocean. In addition, the northwestern part of the Tibetan Plateau, along the Himalaya mountains, also has more cumulus. But, the seasonal variations of the global patterns of cumulus occurrence are small. For the diurnal variation of cumulus (Fig. 2a5), it is clear that

Title Page	
Abstract	Introduction
Conclusions	References
Tables	Figures
◀	▶
◀	▶
Back	Close
Full Screen / Esc	
Printer-friendly Version	
Interactive Discussion	



Distributions and overlap of various cloud types

J. Li et al.

Title Page

Abstract

Introduction

Conclusions

References

Tables

Figures

◀

▶

◀

▶

Back

Close

Full Screen / Esc

Printer-friendly Version

Interactive Discussion



higher frequencies of cumulus during day compared to night are mainly seen over land, especially over central Africa and the northern part of equatorial central South America, where the difference in cumulus fraction between day and night can reach 20 %. The diurnal variation of cumulus fraction is smaller over ocean than over land, the differences do not exceed 5 %. In other words, cumulus cloud fractions tend to exhibit positive difference between night- and daytime over ocean, and negative difference over land.

The other two main precipitating cloud distributions (Ns and Dc) are showed in the Fig. 1a6–d6 and 1a7–d7. Similar with the reports by surface observers, the Ns clouds are primarily located in mid and high latitudes (Warren et al., 1986, 1988). Seasonal variations of global patterns are not apparent. Over mid-latitudes oceans, diurnal Ns effects seem to alternate between day and night (Fig. 2a6). However, deep convective clouds (Dc) are found mainly in the tropics but extend into the mid-latitudes. Actually, their distributions tend to concentrate at the inter-tropical convergence zone, and are thus very important for correct estimations of radiative and latent heat as well as precipitation over this region. Figure 2a7 indicates a complex pattern of diurnal Dc variability over both land and ocean. The complex pattern of diurnal Dc variability is not consistent with recent studies (Sato et al., 2009; Behrangi et al., 2012), which indicated strong evidence for an oceanic night maximum in deep convective clouds. Sassen et al. (2009) showed that more extended observations and studies are needed to better grasp the complex variability in convective activity that could be tied to local terrain and weather interactions. In a word, seasonal and diurnal variations of total cloud fraction (Figs. 1a8–d8 and 2a8) mainly depend on the respective contribution of each cloud type.

3.2 Zonal distributions of each cloud type

The seasonal variations of zonal distributions for different cloud types over land and ocean during day- and night-time are provided in the Fig. 3. Lines with different colors represent different seasons. In Fig. 3, from left to right, the columns represent the zonal averaged cloud fraction of each cloud type over land (day), land (night), ocean

Distributions and
overlap of various
cloud types

J. Li et al.

Title Page

Abstract

Introduction

Conclusions

References

Tables

Figures

◀

▶

◀

▶

Back

Close

Full Screen / Esc

Printer-friendly Version

Interactive Discussion



most of the deep convective clouds or high clouds in our study almost are located in the tropics of the Northern Hemisphere except during winter. It is mainly due to the large thermal inertia and dynamical inertia of the wind-forced surface current structure of the equatorial ocean, the ITCZ migration over extended ocean regions lags slightly behind the ITCZs over land, particularly in the eastern Pacific and the Atlantic oceans (see Fig. 1a7–d7). As a result, the ITCZs over the ocean tend to favor the Northern Hemisphere at most longitudes result in the large-scale convection cloud band also tends to favor the Northern Hemisphere with prevailing warm SSTs (Waliser and Gautier, 1993; Behrangi et al., 2012).

10 4 Comparisons of different cloud type-fractions based on different datasets

4.1 Statistical comparison of global averages

Several cloud classification products based on passive observational datasets (typically ISCCP) and surface observer have been widely used to investigate the global or regional cloud climatologies (e.g. Hahn and Warren, 1999; Rossow and Schiffer, 1999; Yu et al., 2004). The cloud types identified by the remote sensing are basically different from the cloud forms identified by surface observation. Such as, the ISCCP uses a combination of cloud top pressure and cloud optical depth to classify clouds into cumulus, stratocumulus, stratus, altocumulus, altostratus, nimbostratus, cirrus/cirrostratus, and deep convective clouds. However, surface weather reporters classify clouds based on their visual texture and approximate cloud base height by using reporters' knowledge and experiences. Sassen and Wang (2008) preliminarily compared Radar-only based cloud classification (that is, 2B-CLDCLASS dataset from CloudSat) with the cloud classification records from ISCCP and surface observer reports, and showed overall consistency among these datasets.

Following the study of Sassen and Wang (2008), we further compare the global averaged cloud fractions for different cloud types by using four different datasets (see

Distributions and overlap of various cloud types

J. Li et al.

[Title Page](#)

[Abstract](#)

[Introduction](#)

[Conclusions](#)

[References](#)

[Tables](#)

[Figures](#)

◀

▶

◀

▶

[Back](#)

[Close](#)

[Full Screen / Esc](#)

[Printer-friendly Version](#)

[Interactive Discussion](#)



Table 1). One of them is based on extended surface observer reports (Hahn and Warren, 1999), another one on ISCCP satellite observations from 1986–1993 (Rossow and Schiffer, 1999), a third dataset is the Radar-only cloud classification from CloudSat, that is 2B-CLDCLASS product (from June 2006–June 2007), and the last one is the Radar-Lidar cloud classification from CloudSat, that is 2B-CLDCLASS–Lidar product (2007–2010). Here, the statistical results of the former three datasets in the Table 1 are all obtained from the study of Sassen and Wang (2008) (see Table 1 in their paper). These global mean values for each cloud type over land and ocean are cited and used to compare with our statistical findings based on the latest dataset of CloudSat. Since lidar has considerably better sensitivity to high clouds and better vertical resolution than that of CPR, it is more suitable for providing high/middle or geometrically/optically thin cloud profiling and fine cloud structure (such as, cumulus, stratocumulus and altocumulus). From our results (Table 1), it is clear that more high clouds, altocumulus, stratocumulus or stratus and cumulus are identified by the Radar-Lidar cloud classification, in particular for high clouds and cumulus with cloud fractions higher than in previous results based on Radar-only cloud classification, increasing by factors about 2.5 and 4–7, respectively. Generally speaking, compared to the results from Radar-only cloud classification, the new results from Radar-Lidar cloud classification are in more reasonable agreement with at least one of the other datasets, typically ISCCP. By analyzing and comparing the zonal distributions of different cloud types for different datasets (see the Fig. 2 of Sassen and Wang (2008) and Fig. 4 in this paper), we find that the zonal patterns are very similar between 2B-CLDCLASS–Lidar dataset and ISCCP for high clouds, altostratus and deep convective clouds, but the magnitudes are different, especially for the high cloud fractions (ISCCP miss high clouds by 35 % and 25 % over land and ocean, respectively, in the tropics). However, the zonal distributions of other cloud types (such as, altocumulus, stratocumulus or stratus, cumulus and nimbostratus) from 2B-CLDCLASS–Lidar dataset are similar with the patterns from surface observer reports, even for the magnitudes. It is worth noted that we just give a rough comparison about the global mean values of each cloud type based on several

Title Page	
Abstract	Introduction
Conclusions	References
Tables	Figures
◀	▶
◀	▶
Back	Close
Full Screen / Esc	
Printer-friendly Version	
Interactive Discussion	



datasets, the more detailed comparison (such as, grid level) likely be required in future researches.

The overall agreement among the several cloud classifications is what we hope to see, but some difference in the results from several datasets still are inevitable because of different approaches and limitations. For surface observer reports, there are several important biases have to be considered. The ground observers cannot detect cirrus and altostratus when they are present at night, which is referred to as “night detection bias”. Another bias is the underestimation of the frequency of upper clouds due to the possibility that an upper cloud is present behind a partial lower cloud cover yet reported absent because it does not intrude into the region of the sky which is visible through the lower layer. This bias is referred to as “partial under-cast bias” (Warren et al., 1985). For passive satellite products (such as, ISCCP), an apparent drawback of their cloud classification is its dependence on only cloud top information in the cloud classification process. For example, when a high-level transparent cirrus cloud overlies a boundary layer stratus cloud, the retrieved cloud top heights typically lie between the cirrus and the stratus cloud heights (e.g., Baum and Wielicki, 1994) leading to mis-assignment of cloud types by passive satellites. Therefore, the performance of the cloud classification algorithm will be affected by the presence of multilayer clouds. In addition, very thin cirrus can be detected from satellites due to their low temperature, even though it is not thick enough to be seen in reflected sunlight in visible channels. Some of these clouds are “subvisible” and also will always be missed by surface reports (Sassen and Cho, 1992) and underestimated by the ISCCP (Liao et al., 1995). For the active sensors, the poor spatial coverage and short lifetime are possible limitations, which may eventually contribute to the cloud fraction differences for different cloud types between these four datasets. But, it is clear that the limitations of passive observations and contradictions of passive observation differences based on different perspective (above vs. below) can be reconciled largely by using the ranging capabilities of active sensors and their enough sensitivity to optically thin clouds (see Table 1). Especially, the vertical distribution of different cloud types from active sensors can provide us more useful information,

Distributions and overlap of various cloud types

J. Li et al.

[Title Page](#)

[Abstract](#)

[Introduction](#)

[Conclusions](#)

[References](#)

[Tables](#)

[Figures](#)

◀

▶

◀

▶

[Back](#)

[Close](#)

[Full Screen / Esc](#)

[Printer-friendly Version](#)

[Interactive Discussion](#)



Title Page	
Abstract	Introduction
Conclusions	References
Tables	Figures
◀	▶
◀	▶
Back	Close
Full Screen / Esc	
Printer-friendly Version	
Interactive Discussion	



this is very difficult to be obtained from passive satellites and surface weather reports on a global scale before the launch of the CloudSat and CALIPSO. Therefore, as described by the Hahn et al. (2001), a comparison of cloud types determined from surface observations to those obtained from satellite observations provides an assessment of the importance of the differences in perspective (above vs. below), spatial resolution, field of view, and nature of the data (radiometric vs. visual).

4.2 The distributions of dominant cloud types

Figure 4 shows that the global distributions of the most frequent cloud type and corresponding cloud fractions during day- and night-time. It is evident from Fig. 4 that stratus and stratocumulus are the dominant cloud types worldwide, particularly over the ocean. High clouds are mainly concentrated in the tropics and subtropics. In addition, over Antarctica, the most frequent cloud type is altostratus except for a small difference between day and night-time. These results are in reasonable agreement with the findings based on the ISCCP D1 dataset (Doutriaux-Boucher and Seze, 1998). But, Fig. 4 shows that altostratus also prevails over the arid/semi-arid land in the Northern Hemisphere, such as, the northwestern part of China and North America. In contrast, altocumulus is the dominant cloud type over the arid/semi-arid land of the Southern Hemisphere, such as Australia and the southern part of Africa. However, all these features are not observed by Doutriaux-Boucher and Seze (1998) using the ISCCP D1 dataset. It is certain that these middle clouds are often of mixed-phase composition means that any cloud layer temperature change will affect the balance of their phases (ice or water or mixed) with a potentially large radiative impact in local regions (Sassen and Khvorostyanov, 2007). In addition, over some deserts (such as the Sahara Desert), the most prevalent cloud type is a low level cloud (stratocumulus and stratus) in ISCCP D1 rather than a high cloud in our results. This discrepancy may be due to inadequate identification of airborne dust as low level clouds by ISCCP, as suggested by the low values of effective droplet radius reported by Han et al. (1994) over these regions.

However, it is worth further noting that the cloud fractions of different cloud types in the above analyses, including single-layer and multilayered cloud fractions for certain types, are referred to as the total cloud fraction of each cloud type.

5 Simultaneous occurrence of different cloud types

- 5 Multilayered cloud systems, with two or more cloud types occurring simultaneously over the same location but at different levels in the atmosphere have been frequently reported by surface and aircraft observations (Tian and Curry, 1989). The effects of individual clouds on the surface and atmospheric radiation budgets depend on whether other clouds are also present above or below them. In this section, we will mainly
10 discuss the co-occurrence frequencies of different cloud types and evaluate the performance of overlap assumptions by using the new dataset.

5.1 Zonal distributions and global statistics of co-occurrence frequency of different cloud types

- By detailed analysis, we further pick out the annual most frequently multi-layered cloud
15 systems and provide their zonal distributions during day- and night-time (Fig. 5a–d) and their zonal differences between land and ocean (Fig. 5e–h). Figure 5a–d clearly indicate that the zonal patterns of different combinations of cloud types are very different. For example, multilayered cloud systems which include high clouds either have one peak in the tropics (High + High, High + Ac and High + Cu) or three peaks in the tropics
20 and mid-latitudes (High + St/Sc, High + Ns and High + As). The high clouds in the major peak in the tropics may be caused by the large-scale ascent or by the dissipating deep convection. However, gentle large-scale ascent and ice cloud production from frontal convection are likely responsible for the two minor peaks of multilayered cloud systems in the mid-latitudes storm tracks (Yuan and Oreopoulos, 2013). Besides these combinations of cloud types, As-over-strati-form clouds or Ac-over-strati-form clouds also

Distributions and overlap of various cloud types

J. Li et al.

[Title Page](#)

[Abstract](#)

[Introduction](#)

[Conclusions](#)

[References](#)

[Tables](#)

[Figures](#)

◀

▶

◀

▶

[Back](#)

[Close](#)

[Full Screen / Esc](#)

[Printer-friendly Version](#)

[Interactive Discussion](#)



tend to concentrate in the mid-latitudes (60° and pole-ward). In fact, the distributional patterns of cloud in different geographical regimes may depend on environmental factors in these regimes, such as sea surface temperature, lower tropospheric stability, and vertical velocity (Norris and Leovy, 1994; Klein and Hartmann, 1993). In recent work, by studying the relations between various cloud types and sea surface temperature over the tropical oceans, Behrangi et al. (2012) indicated that as SST increases, the fraction of multilayered clouds increases up to an SST of 303 K, and then decreases for SSTs greater than 303 K. For different combinations of cloud types, high cloud over strati-form or nimbostratus tend to occur between 292 and 294 K, but high cloud over altocumulus or altostratus or cumulus tend to exist between 302 and 304 K even though almost all of them have major peak values in the tropics. However, other combinations (such as Ac-over-strati-form clouds or As-over-strati-form clouds) are more likely to occur over the ocean with SST between 298 and 300 K or between 302 and 304 K. In addition, Yuan and Oreopoulos (2013) further indicated that large-scale pressure vertical velocity is found to anti-correlate well with the percentage of multilayered cloud systems. Strong subsidence thus favors low cloud formation and suppresses ice cloud generation, explaining why multilayered clouds are very infrequent over major stratocumulus dominated oceanic areas around 30° latitude. Further, cloud fraction differences between land and ocean for these multi-layered cloud systems are non-negligible, and the zonal differences during daytime are also apparently different compared to the results obtained during night, especially for high-over-Cu and high-over-St/Sc.

Global average overlapping percentages of different combinations of cloud types over land and ocean during daytime and nighttime are provided in Tables 2 and 3, respectively. These tables show that high cloud, As, Ac and cumulus types are much more likely to co-exist with other cloud types regardless of day or night, land or ocean. The frequency of high-over-Ac even may exceed the frequency of single-layered altocumulus cloud, indicating that these two types actually exhibit a stronger meteorological association. However, due to under large-scale subsidence regions, stratus/stratocumulus and nimbostratus are much more likely to exhibit individualism fea-

[Title Page](#)[Abstract](#)[Introduction](#)[Conclusions](#)[References](#)[Tables](#)[Figures](#)[|◀](#)[▶|](#)[◀](#)[▶](#)[Back](#)[Close](#)[Full Screen / Esc](#)[Printer-friendly Version](#)[Interactive Discussion](#)

Distributions and overlap of various cloud types

J. Li et al.

Title Page

Abstract

Introduction

Conclusions

References

Tables

Figures

◀

▶

Back

Close

Full Screen / Esc

Printer-friendly Version

Interactive Discussion



tures, particularly for stratus/stratocumulus over the ocean. For convective clouds, they are also typically single. Although cumulus occurs in unstable air whereas altostratus occurs in stable air, there is still a small percentage of overlap between them. Globally, 44 % (50 %) and 35 % (39 %) of low clouds (St/Sc + Cu) over land and ocean during daytime (nighttime) are overlapped by other cloud types aloft, respectively. About 23 % (26 %) and 20 % (25 %) of low clouds over land and ocean during daytime (nighttime) are connected with high clouds, respectively. These percentages are comparable with those (about 30 %) provided by Yuan and Oreopoulos (2013). Deep convective clouds are predominantly concentrated in the equatorial region, and account for about 1.1 % of total observations. Previous studies have shown that tropical cirrus clouds can be stacked above deep convection (Garrett et al., 2004; Wang and Dessler, 2006), and sufficient overlapping can lead to net radiative cooling accompanied by subsidence and contribute to a mechanism for drying the air entering the stratosphere (Wang and Dessler, 2006; Hartmann et al., 2001). In our study, it is worth noting that high clouds also include cirrostratus and cirrocumulus, thus the overlap fraction of deep convection lying below high clouds is about 29 %, and larger than the fraction (about 24 %) of cirrus-over-convection clouds based on ICESat/GLAS (Geoscience Laser Altimeter System) (Wang and Dessler, 2006).

Based on above figures and tables, we further plot the global distributions of annual mean dominant multiple cloud types during day- and night-time (see Fig. 6). Generally speaking, the patterns are similar between day and night. Figure 6b and d show the multilayered cloud-type amount, defined as the ratio of the cloud fraction of one multilayered cloud combination to the cloud fraction of total multilayered cloud systems. In addition, we note that there is still some multilayered cloud systems (almost is high-over-St/Sc) over the major stratocumulus dominated oceanic areas, which are generally unfavorable to upper level cloud formation due to persistent strong subsidence. The major source of high cloud is topography-driven gravity wave activity, advection from neighboring tropical convection centers such as the Amazon Basin, the Congo Basin, or ascent associated with mid-latitude fronts (Yuan and Oreopoulos, 2013).

5.2 Evaluation of cloud overlap assumptions based on cloud types

The cloud overlap assumption has been widely used to describe the real cloud vertical distribution and parameterization of the total cloud fraction in a given model grid box. Several basic cloud overlap assumptions have been proposed, such as, maximum, random, random-maximum and minimum overlap (Hogan and Illingworth, 2000). However, the choice of overlap assumption in GCMs could result in errors in instantaneous solar flux estimates on the order of several hundred W m^{-2} (Baker et al., 1999). The most common cloud overlap scheme in current GCMs is called “random-maximum” overlap. It assumes that cloud layers separated by any clear layers are randomly overlapped while vertically-continuous cloud layers overlap maximally (Stephens et al., 2004). If given the cloud fractions of upper and lower layers as C_1 and C_2 , the total cloud fractions of the two cloud layers based on these overlap assumptions thus are given by:

$$\begin{aligned} C_{\text{random}} &= C_1 + C_2 - C_1 \cdot C_2, \\ C_{\text{max}} &= \max(C_1, C_2), \text{ and} \\ C_{\text{min}} &= \min(1, C_1 + C_2). \end{aligned} \quad (1)$$

In addition, if we know the real overlap fraction C_{overlap} , then the observed total cloud fraction C_{real} can be written as:

$$C_{\text{real}} = C_1 + C_2 - C_{\text{overlap}} \quad (2)$$

However, Hogan and Illingworth (2000) showed that contrary to the assumption made in most models, the vertically continuous cloud layers tend not to be maximally overlapped but random overlapped as vertical separation of these two layers is increased. Thus, they proposed a simpler and more useful expression for the degree of cloud layer overlap (that is, exponential random overlap). In the expression, the mean observed cloud fraction of two cloud layers can be determined by the linear combination of maximum and random overlap in terms of an “overlap parameter” a as:

$$C_{\text{real}} = a \cdot C_{\text{max}} + (1 - a) \cdot C_{\text{random}} \quad (3)$$

Title Page	
Abstract	Introduction
Conclusions	References
Tables	Figures
◀	▶
◀	▶
Back	Close
Full Screen / Esc	
Printer-friendly Version	
Interactive Discussion	



Distributions and overlap of various cloud types

J. Li et al.

Here, the overlap parameter a is considered as a function of layer separation. If $a = 0$ corresponds to random overlap and $a = 1$ to maximum overlap. As C_{real} departs more and more from C_{\max} (trends toward C_{\min}), a becomes negative. But, in the case of vertically non-continuous cloud, they indicated that random overlap assumption works well. Based on the several months' data from ICESat/GLAS observations, Wang and Dessler (2006) already evaluated how well random overlap can describe the real overlap of two separated cloud types (vertical separation > 0.5 km). Their results showed that overlap difference between observed and based on random overlap still exist. However, their work only focused on the tropical area and is limited to simple cloud classification based on space-based lidar. To expand their study to the global scale and more complete cloud classification, we plan to follow the study of Wang and Dessler (2006) to further estimate the overlap of two separated cloud types of each combination of different cloud types in each grid box by using the observations of CloudSat and CALIPSO, moreover evaluate the performances of random and maximum overlap assumptions and calculate the overlap parameter a for each multilayered cloud type in each grid box.

In order to do this, we first group each multilayered cloud system. For example, for the High + St/Sc multilayered cloud systems in same grid box, we don't group them into many layers according to the vertical separation of two types for convenience, but only consider two layers and group all high clouds into the upper layer and all strati-from clouds are grouped into the lower layer. Then, four possible values for the combined cloud fraction of the two cloud types at different layers are calculated by assuming random overlap, maximum overlap, minimum overlap and actually observed. In view of random cloud overlap is extensively thought to better characterize cloud overlap behavior than minimum overlap and maximum overlap, here we only provide the difference of cloud fraction between random overlap and actually observed. At last, the overlap parameter a for each multilayered cloud types in each grid will be calculated based on the Eq. (3). However, it is worth noting that due to we don't group multilayered cloud types into many layers according to the vertical separation of two types, thus

Title Page	
Abstract	Introduction
Conclusions	References
Tables	Figures
◀	▶
◀	▶
Back	Close
Full Screen / Esc	
Printer-friendly Version	
Interactive Discussion	



only one value of overlap parameter a for each multilayered cloud system in each grid is obtained. The a may be considered as the mean value of all overlap parameters at different layer separation. Based on above consideration, we use the 2B-CLDCLASS-Lidar product to calculate the four possible values for the combined cloud fraction based on different overlap assumptions, and evaluate cloud overlap schemes used by GCMs. Here, the relative difference (RD) between random and real overlap for one of the multilayered cloud types is defined as:

$$RD = (C_{\text{random}} - C_{\text{real}})/C_{\text{real}} \quad (4)$$

In addition, the cumulative relative difference (CRD) between random and real overlap for all multilayered cloud types (about 17 different combinations of different cloud types) in each $2^\circ \times 2^\circ$ grid box is given by:

$$\text{CRD} = \sum_{i=1}^{17} RD^i \cdot w^i \quad i = 1, 2, 3, \dots, 17 \quad (5)$$

Similar with the definition of CRD, we define cumulative overlap parameter (COP) in each $2^\circ \times 2^\circ$ grid box as:

$$\text{COP} = \sum_{i=1}^{17} a^i \cdot w^i \quad i = 1, 2, 3, \dots, 17 \quad (6)$$

where w is the weight coefficient for one of multilayered cloud types in each $2^\circ \times 2^\circ$ grid box. It can be written as follows:

$$w^i = f^i / (\sum_{i=1}^{17} f^i) \quad i = 1, 2, 3, \dots, 17 \quad (7)$$

where f is the cloud fraction of each multilayered cloud type in every grid box.

Distributions and overlap of various cloud types

J. Li et al.

[Title Page](#)

[Abstract](#)

[Introduction](#)

[Conclusions](#)

[References](#)

[Tables](#)

[Figures](#)

[|◀](#)

[▶|](#)

[◀](#)

[▶](#)

[Back](#)

[Close](#)

[Full Screen / Esc](#)

[Printer-friendly Version](#)

[Interactive Discussion](#)



Figure 7 shows the zonal distributions of the relative difference for ten of the main multilayered cloud types and the cumulative relative difference of all multilayered cloud types during day- and night-time. The results show that differences still exist even if random cloud overlap assumption is thought to better describe cloud overlap behavior

5 than other schemes when the cloud layers appear to be separated. The cloud fractions based on the random overlap assumption are underestimated for High + St/Sc, As+St/Sc and Ac+St/Sc at all latitudes. These differences even exceed –5 %. Among these types, a negative difference is also obvious for Ac + St/Sc, especially at the
10 Nothern Hemisphere. The cloud fraction of high-over-altocumulus system is overestimated at all latitudes. The peak values of difference are mainly located at mid- and high- latitudes in both Hemispheres and can reach 5 %. For other types, the relative differences are smaller than for the above four types, and alternate with latitudes. In
15 summary, the cumulative relative difference of all multilayered cloud types is small (gray lines), and almost is negative at the all latitudes. In the Fig. 8, we further show the zonal distributions of overlap parameter for ten of the main multilayered cloud types and the cumulative overlap parameter of all multilayered cloud types during day- and night-time.
20 It is clear that the overlap parameters for High + St/Sc, As + St/Sc and Ac + St/Sc at all latitudes all are negative, indicate that their C_{real} depart from C_{max} (trend toward C_{min}) and a tendency for an even lower degree of overlap than that predicted by the
25 random overlap assumption. Thus, the linear combination of maximum and random overlap assumptions, which has an exponential parameterization of overlap parameter a , possible are problematic due to negative overlap parameters at those regions, where above three multilayered cloud types are dominant, especially over the major stratocumulus dominated oceanic areas where the High + St/Sc accounts for 80 % of multilayered cloud. However, the overlap parameters almost are positive for High +Ns and High + Ac. This indicates that their C_{real} more trend to take values anywhere between the C_{max} and C_{random} , thus the exponential random overlap can predict the real overlap of these two types very well. For other multilayered cloud types, the overlap parameters alternate with latitudes. In summary, the cumulative overlap parameters

Distributions and overlap of various cloud types

J. Li et al.

[Title Page](#)

[Abstract](#)

[Introduction](#)

[Conclusions](#)

[References](#)

[Tables](#)

[Figures](#)

◀

▶

◀

▶

[Back](#)

[Close](#)

[Full Screen / Esc](#)

[Printer-friendly Version](#)

[Interactive Discussion](#)



of all multilayered cloud types (gray lines) almost are negative at the all latitudes. But, there are two points still need to be further interpreted. First, the cumulative overlap parameters at tropics and Nouthern Hemisphere have small values (even have positive values), thus random overlap or exponential random overlap still can works well. Second, at the Southern Hemisphere, the cumulative overlap parameters become larger and more trend toward C_{\min} , thus it is difficult to provide better prediction by using the random overlap or exponential random overlap. Based on these results, we suggest that a linear combination of minimum and random overlap assumptions possible may further improve the predictions of real cloud fraction for those multilayered cloud types at the Southern Hemisphere (e.g. As+St/Sc and Ac+St/Sc), especially over the ocean of 40° S pole-ward. These results also further indicate that incorporating co-occurrence information of different cloud types on a global scale by using Radar-Lidar cloud classification into the overlap assumption schemes used in the current GCMs possible be able to provide an better predictions for vertically projected total cloud fraction.

The global distributions of the cumulative relative difference and the cumulative overlap parameter for all multilayered cloud types during day- and night-time are shown in Fig. 9. The upper panels of this figure are for the cumulative relative difference, whereas the lower panels are for the cumulative overlap parameter. Based on the upper panels of this figure, we find that the cloud fractions based on random overlap assumption main are underestimated over the vast ocean except the west-central Pacific Ocean warm pool. Obvious overestimations are mainly located at the lands of tropics and subtropics, particularly at the regions with low multilayered cloud fraction, such as equatorial central South America, southern and northern Africa, Australia and the Antarctic continent, where the high-over-altocumulus system is the dominant multilayered cloud type. This pattern indicates that land surface effects may favor an exponential random overlap (ERO). Based on Figs. 7 and 9, the cumulative relative difference still is small even if some multilayered cloud types are apparently over- and underestimated by random overlap. This main is due to the lower weight of them or the differences are canceled out to some extent. In the lower panels of this figure, the distributions of

Title Page	
Abstract	Introduction
Conclusions	References
Tables	Figures
◀	▶
◀	▶
Back	Close
Full Screen / Esc	
Printer-friendly Version	
Interactive Discussion	



Distributions and
overlap of various
cloud types

J. Li et al.

Title Page

Abstract

Introduction

Conclusions

References

Tables

Figures

◀

▶

◀

▶

Back

Close

Full Screen / Esc

Printer-friendly Version

Interactive Discussion



the cumulative overlap parameter are similar with those results of cumulative relative difference. Negative overlap parameters also mainly occur over the vast ocean except the west-central Pacific Ocean warm pool. The typical negative high-values centers are correspondence with the major stratocumulus dominated oceanic areas very well. The

positive overlap parameters almost locate the lands of tropics and subtropics and the Antarctic continent.

Finally, Tables 4 and 5 provide the global statistical results of several important multi-layered cloud types during day- and night-time. Globally, by using the random overlap, the overlap fractions are overestimated by 19 %, 29.6 %, 81.5 % and 116 % for high clouds with strati-form clouds and deep convective, or altostratus and altocumulus with strati-form clouds over land during daytime, respectively. The overestimation also happens for altostratus or altocumulus over cumulus. However, the overlap of high cloud with altocumulus and cumulus are underestimated by 28.7 % and –8.9 % over land during daytime, respectively. It is clear that the overlap differences are obviously different between land and ocean. For nighttime, the difference of overlap fractions are more complicated. In summary, the difference between C_{overlap} and C_{real} are more obvious for high cloud over altocumulus, strati-form clouds and altocumulus over strati-form clouds.

6 Summary and discussion

Since the cloud types and their co-occurrence variations are the most significant components of the global climate system and cloud climatology studies, GCMs are difficult to make correct climate predictions before cloud types and cloud overlap have not been completely depicted by observations and further reasonably represented in the models. By using the ranging capabilities of active sensors, we analyze the geographical distributions of different cloud types and their co-occurrence frequency across different seasons and further evaluate the cloud overlap assumptions based on 4 year' Radar-Lidar cloud classification product from CloudSat. Although some statistical results are

Distributions and overlap of various cloud types

J. Li et al.

[Title Page](#)[Abstract](#)[Introduction](#)[Conclusions](#)[References](#)[Tables](#)[Figures](#)[|](#)[|](#)[◀](#)[▶](#)[Back](#)[Close](#)[Full Screen / Esc](#)[Printer-friendly Version](#)[Interactive Discussion](#)

in reasonable agreement with previous works, additional new insights are gained in this paper.

By using 2B-CLDCLASS–Lidar dataset, more high clouds, altocumulus, stratocumulus or stratus and cumulus are identified by the Radar-Lidar cloud classification.

In particular for high clouds and cumulus, the cloud fractions are higher than shown in previous results by a factor of 2.5 and 4–7, respectively. Compared to the results from Radar-only cloud classification, the new results from Radar-Lidar cloud classification are in more reasonable agreement with at least one of the other datasets, typically ISCCP. The global distributions of the most frequent cloud types show that stratocumulus and stratus are the dominant cloud types worldwide, particularly over the ocean. However, high clouds are mainly concentrated in the tropics and subtropics. These results are agreement with the findings based on the ISCCP D1 dataset (Doutriaux-Boucher and Seze, 1998). In addition, we also find some features, which weren't observed by Doutriaux-Boucher and Seze (1998) using the ISCCP D1 dataset.

For example, altostratus and altocumulus prevail over the arid/semi-arid land of the Northern Hemisphere (northwestern part of China and North America) and the Southern Hemisphere (Australia and the southern part of Africa), respectively. Besides these, over some deserts (such as Sahara Desert), the most prevalent cloud type is a low level cloud (stratocumulus and stratus) in ISCCP D1 rather than a high cloud in our results.

The statistical results clearly show that the zonal patterns of different combinations of cloud types are very different due to different environmental factors, such as sea surface temperature, lower tropospheric stability and vertical velocity. The high cloud, altostratus, altocumulus and cumulus types are much more likely to co-exist with other cloud types regardless of day or night, land or ocean. However, the stratus/stratocumulus and nimbostratus, which typically are under large-scale subsidence regions, and convective clouds are much more likely to be caused by individual features, particularly for stratus/stratocumulus over the ocean. Finally, we also evaluated how well the overlap assumptions can describe the real overlap of two separated cloud types, and calculate the overlap parameter in the exponential random overlap for each

Distributions and
overlap of various
cloud types

J. Li et al.

Title Page

Abstract

Introduction

Conclusions

References

Tables

Figures

◀

▶

Back

Close

Full Screen / Esc

Printer-friendly Version

Interactive Discussion



multilayered cloud type in each grid box by using the 2B-CLDCLASS–Lidar dataset. The results show that differences still exist even if the random cloud overlap assumption is thought to better describe cloud overlap behavior than other schemes for two separated cloud layers or types. In summary, the cloud fractions based on the random overlap assumption mainly leads to an underestimation over the vast ocean except for the west-central Pacific Ocean warm pool. Obvious overestimations are primarily occurring in the lands areas of the tropics and subtropics, particularly in regions with low multilayered cloud fractions. The global distributions of the cumulative overlap parameter are similar with those results of cumulative relative difference. Negative overlap parameters also main occur over the vast ocean, especially over the ocean of 40° S pole-ward. We suggest that a linear combination of minimum and random overlap assumptions possible may further improve the predictions of real cloud fraction for those multilayered cloud types (e.g. As + St/Sc and Ac + St/Sc) at these regions. However, the positive overlap parameters almost locate the lands of tropics and subtropics and the Antarctic continent, it indicates that random overlap or exponential random overlap still can works well at these areas. Thus, by incorporating co-occurrence information of different cloud types on a global scale based on Radar-Lidar cloud classification into the overlap assumption schemes used in the current GCMs possible be able to provide an better predictions for vertically projected total cloud fraction.

Since different cloud types, resulting from different meteorological processes, have different effects on radiation fluxes, we emphasize the importance of examining distributions in individual cloud types and their co-occurrence frequencies. A previous study (Li et al., 2011) has indicated that multilayered clouds have a significant impact on the radiation budget which evidently differs from that of single-layered clouds, especially in the tropics. It is expected that this difference mainly is due to the net radiative impact of the different cloud types within one multilayered cloud system which possibly cancel out at the top of atmosphere to some extent. But, no study has determined the extent and combination of cloud types responsible for the difference in radiative forcing between single-layered and multilayered clouds, especially in the tropics. Based on the

statistical results in part I, we will further focus on these issues and give more detailed analyses and interprets in the part II. In addition, although the interactions between aerosol and cloud in some typical regions (such as, arid/semi-arid regions or monsoon areas) have been widely investigated (Huang et al., 2006b; Su et al., 2008; Wang et al., 2010), whereas the related information with cloud types still needed to be considered in order to better quantify the feedback of an individual cloud type (especially middle clouds, such as altostratus or altocumulus) to these regions and document the local cloud climatology.

Acknowledgements. This research was supported jointly supported by the National Basic Research Program of China under No. 2013CB955802, No. 2012CB955301 and National Science Foundation of China under grant 41205015. We also would like to thank the CALIPSO, and CloudSat science teams for providing excellent and accessible data products that made this study possible.

References

- 15 Ackerman, T. P., Liou, K. N., Valero, F. P. J., and Pfister, L.: Heating rates in tropical anvils, *J. Atmos. Sci.*, 45, 1606–1623, 1988.
- Barker, H. W.: Overlap of fractional cloud for radiation calculations in GCMs: a global analysis using CloudSat and CALIPSO data, *J. Geophys. Res.*, 113, D00A01, doi:10.1029/2007JD009677, 2008.
- 20 Barker, H. W., Stephens, G. L., and Fu, Q.: The sensitivity of domain averaged solar fluxes to assumptions about cloud geometry, *Q. J. Roy. Meteor. Soc.*, 125, 2127–2152, 1999.
- Baum, B. A. and Wielicki, B. A.: Cirrus cloud retrieval using infrared sounding data: multilevel cloud errors, *J. Appl. Meteorol.*, 33, 107–117, 1994.
- Behrangi, A., Kubasik, T., and Lambrightsen, B. H.: Phenomenological description of tropical clouds using CloudSat cloud classification, *Mon. Weather Rev.*, 140, 3235–3249, 2012.
- 25 Bergman, J. W. and Salby, M. L.: Diurnal variations of cloud cover and their relationship to climatological conditions, *J. Climate*, 9, 2802–2820, 1996.
- Betts, A. K. and Boers, R.: A cloudiness transition in a marine boundary layer, *J. Atmos. Sci.*, 47, 1480–1497, 1990.

ACPD

14, 10463–10514, 2014

Distributions and overlap of various cloud types

J. Li et al.

Title Page

Abstract

Introduction

Conclusions

References

Tables

Figures

◀

▶

◀

▶

Back

Close

Full Screen / Esc

Printer-friendly Version

Interactive Discussion



Distributions and overlap of various cloud types

J. Li et al.

[Title Page](#)

[Abstract](#)

[Introduction](#)

[Conclusions](#)

[References](#)

[Tables](#)

[Figures](#)

◀

▶

◀

▶

[Back](#)

[Close](#)

[Full Screen / Esc](#)

[Printer-friendly Version](#)

[Interactive Discussion](#)



Distributions and
overlap of various
cloud types

J. Li et al.

- Hahn, C. J. and Warren, S. G.: Extended Edited Cloud Reports From Ships and Land Stations Over the Globe, 1952–1996, Numer. Data Package NDP-026C, 79 pp., Carbon Dioxide Inf. Anal. Cent., Dep. of Energy, Oak Ridge, Tenn, 1999.
- Hahn, C. J., Rossow, W. B., and Warren, S. G.: ISCCP cloud properties associated with standard cloud types identified in individual surface observations, *J. Climate*, 14, 11–28, 2001.
- 5 Han, Q., Rossow, W. B., and Lacis, A. A.: Near-global survey of effective droplet radii in liquid water clouds using ISCCP data, *J. Climate*, 7, 465–497, 1994.
- Hartmann, D. L., Ockert-Bell, M. E., and Michelsen, M. L.: The effect of cloud type on Earth's energy balance: global analysis, *J. Climate*, 5, 1281–1304, 1992.
- 10 Hartmann, D. L., Holton, J. R., and Fu, Q.: The heat balance of the tropical tropopause, cirrus and stratospheric dehydration, *Geophys. Res. Lett.*, 28, 1969–1972, 2001.
- Hogan, R. J. and Illingworth, A. J.: Deriving cloud overlap statistics from radar, *Q. J. Roy. Meteor. Soc.*, 128, 2903–2909, 2000.
- 15 Hu, Y., Rodier, S., Xu, K., Sun, W., Huang, J., Lin, B., Zhai, P., and Josset, D.: Occurrence, liquid water content, and fraction of supercooled water clouds from combined CALIOP/IIR/MODIS measurements, *J. Geophys. Res.*, 115, D00H34, doi:10.1029/2009JD012384, 2010.
- Huang, J. P., Minnis, P., and Lin, B.: Advanced retrievals of multilayered cloud properties using multispectral measurements, *J. Geophys. Res.*, 110, D15S18, doi:10.1029/2004JD005101, 2005.
- 20 Huang, J. P., Minnis, P., and Lin, B.: Determination of ice water path in ice-over-water cloud systems using combined MODIS and AMSR-E measurements, *Geophys. Res. Lett.*, 33, L21801, doi:10.1029/2006GL027038, 2006a.
- Huang, J. P., Minnis, P., Lin, B., Wang, T., Yi, Y., Hu, Y., Sun-Mack, S., and Ayers, K.: Possible influences of Asian dust aerosols on cloud properties and radiative forcing observed from 25 MODIS and CERES, *Geophys. Res. Lett.*, 33, L06824, doi:10.1029/2005GL024724, 2006b.
- Kato, S., Sun-Mack, S., Miller, W. F., Rose, F. G., Chen, Y., Minnis, P., and Wielicki, B. A.: Relationships among cloud occurrence frequency, overlap, and effective thickness derived from CALIPSO and CloudSat merged cloud vertical profiles, *J. Geophys. Res.*, 115, D00H28, doi:10.1029/2009JD012277, 2010.
- 30 Klein, S. A. and Hartmann, D. L.: The seasonal cycle of low stratiform clouds, *J. Climate*, 6, 1588–1606, 1993.

Title Page	
Abstract	Introduction
Conclusions	References
Tables	Figures
	
	
Back	Close
Full Screen / Esc	
Printer-friendly Version	
Interactive Discussion	



Distributions and overlap of various cloud types

J. Li et al.

[Title Page](#)

[Abstract](#)

[Introduction](#)

[Conclusions](#)

[References](#)

[Tables](#)

[Figures](#)

◀

▶

◀

▶

[Back](#)

[Close](#)

[Full Screen / Esc](#)

[Printer-friendly Version](#)

[Interactive Discussion](#)



Li, J., Yi, Y., Minnis, P., Huang, J., Yan, H., Ma, Y., Wang, W., and Ayers, K.: Radiative effect differences between multi-layered and single-layer clouds derived from CERES, CALIPSO, and CloudSat data, *J. Quant. Spectrosc. Ra.*, 112, 361–375, 2011.

Liang, X. Z. and Wu, X.: Evaluation of a GCM subgrid cloudradiation interaction parameterization using cloud-resolving model simulations, *Geophys. Res. Lett.*, 32, L06801, doi:10.1029/2004GL022301, 2005.

Liao, X., Rossow, W. B., and Rind, D.: Comparison between SAGE II and ISCCP high-level clouds. Part I: Global and zonal mean cloud amounts, *J. Geophys. Res.*, 100, 1121–1135, 1995.

Luo, Y., Zhang, R., and Wang, H.: Comparing occurrences and vertical structures of hydrometeors between the eastern China and the Indian monsoon region using CloudSat/CALIPSO data, *J. Climate*, 22, 1052–1064, 2009.

Mace, G. G., Deng, M., Soden, B., and Zipser, E.: Association of tropical cirrus in the 10–15-km layer with deep convective sources: an observational study combining millimeter radar data and satellite-derived trajectories, *J. Atmos. Sci.*, 63, 480–503, 2006.

Minnis, P., Ayers, J. K., Palikonda, R., and Phan, D.: Contrails, cirrus trends, and climate, *J. Climate*, 17, 1671–1685, 2004.

Minnis, P., Yi, Y., Huang, J., and Ayers, J. K.: Relationships between radiosonde and RUC-2 meteorological conditions and cloud occurrence determined from ARM data, *J. Geophys. Res.*, 110, D23204, doi:10.1029/2005JD006005, 2005.

Minnis, P., Huang, J., Lin, B., Yi, Y., Arduim, R., Fan, T.-F., Ayers, J. K., and Mace, G. G.: Ice cloud properties in ice-over-water cloud systems using Tropical Rainfall Measuring Mission (TRMM) visible and infrared scanner and TRMM Microwave Imager data, *J. Geophys. Res.*, 112, D06206, doi:10.1029/2006JD007626, 2007.

Moran, J. M., Morgan, M. D., and Pauley, P. M.: *Meteorology: The Atmosphere and the Science of Weather*, Prentice Hall, New Jersey, 530 pp., 1997.

Morcrette, J. J. and Jakob, C.: The response of the ECMWF model to changes in the cloud overlap assumption, *Mon. Weather Rev.*, 128, 1707–1732, 2000.

Norris, J. R.: Low cloud type over the ocean from surface observations. Part II: Geographical and seasonal variations, *J. Climate*, 11, 383–403, 1998.

Norris, J. R. and Leovy, C. B.: Interannual variability in stratiform cloudiness and sea surface temperature, *J. Climate*, 7, 1915–1925, 1994.

Parker, S. P.: *Meteorology Source Book*, McGraw-Hill, New York, 304 pp., 1988.

Distributions and
overlap of various
cloud types

J. Li et al.

Title Page

Abstract

Introduction

Conclusions

References

Tables

Figures

◀

▶

◀

▶

Back Close

Full Screen / Esc

Printer-friendly Version

Interactive Discussion



- Rossow, W. B. and Schiffer, R. A.: ISCCP cloud data products, *B. Am. Meteorol. Soc.*, 72, 2–20, 1991.
- Rossow, W. B. and Schiffer, R. A.: Advances in understanding clouds from ISCCP, *B. Am. Meteorol. Soc.*, 80, 2261–2286, 1999.
- 5 Rozendaal, M. A., Leovy, C. B., and Klein, S. A.: An observational study of the diurnal cycle of marine stratiform cloud, *J. Climate*, 8, 1795–1809, 1995.
- Sassen, K.: Cirrus clouds: a modern perspective, in: *Cirrus*, edited by: Lynch, D. et al., Oxford Univ. Press, New York, 11–40, 2002.
- 10 Sassen, K. and Cho, B. S.: Subvisual–thin cirrus lidar dataset for satellite verification and climatological research, *J. Appl. Meteorol.*, 31, 1275–1285, 1992.
- Sassen, K. and Khvorostyanov, V. I.: Microphysical and radiative properties of mixed phase altocumulus: a model evaluation of glaciation effects, *Atmos. Res.*, 84, 390–398, 2007.
- 15 Sassen, K. and Wang, Z.: Classifying clouds around the globe with the CloudSat radar: 1-year of results, *Geophys. Res. Lett.*, 35, L04805, doi:10.1029/2007GL032591, 2008.
- Sassen, K., Wang, Z., and Liu, D.: The global distribution of cirrus clouds from CloudSat/Cloud-Aerosol Lidar and Infrared Pathfinder Satellite Observations (CALIPSO) measurements, *J. Geophys. Res.*, 113, D0012, doi:10.129/2008JD009972, 2008.
- 20 Sassen, K., Wang, Z., and Liu, D.: Cirrus clouds and deep convection in the tropics: insights from CALIPSO and CloudSat, *J. Geophys. Res.*, 114, D00H06, doi:10.1029/2009JD011916, 2009.
- Sato, T., Miura, H., Satoh, M., Takayabu, Y. N., and Wang, Y. Q.: Diurnal cycle of precipitation in the tropics simulated in a global cloud-resolving model, *J. Climate*, 22, 4809–4826, 2009.
- Stephens, G. L.: Cloud feedbacks in the climate system: a critical review, *J. Climate*, 18, 237–273, 2005.
- 25 Stephens, G. L., Vane, D. G., Boain, R. J., Mace, G. G., Sassen, K., Wang, Z., Illingworth, A. J., O'Connor, E. J., Rossow, W. B., Durden, S. L., Miller, S. D., Austin, R. T., Benedetti, A., Mitrescu, C., and CloudSat Science Team: The CloudSat mission and the A-Train, a new dimension of space-based observations of clouds and precipitation, *B. Am. Meteorol. Soc.*, 83, 1771–1790, 2002.
- 30 Stephens, G. L., Wood, N. B., and Gabriel, P. M.: An assessment of the parameterization of subgrid-scale cloud effects on radiative transfer: Part I. Vertical overlap, *J. Atmos. Sci.*, 61, 715–732, 2004.

Distributions and overlap of various cloud types

J. Li et al.

[Title Page](#)

[Abstract](#)

[Introduction](#)

[Conclusions](#)

[References](#)

[Tables](#)

[Figures](#)

◀

▶

◀

▶

[Back](#)

[Close](#)

[Full Screen / Esc](#)

[Printer-friendly Version](#)

[Interactive Discussion](#)



Distributions and
overlap of various
cloud types

J. Li et al.

- World Meteorological Organization: International Cloud Atlas: Abridged Atlas, World Meteorological Organization, 62 pp., and 72 plates, Geneva, 1956.
- Xu, H., Wang, Y., and Xie, S. P.: Effects of the Andes on eastern Pacific climate: a regional atmospheric model study, *J. Climate*, 17, 589–602, 2004.
- 5 Yu, H., Remer, L. A., Chin, M., Bian, H., Tan, Q., Yuan, T., and Zhang, Y.: Aerosols from overseas rival domestic emissions over North America, *Science*, 337, 566–569, doi:10.1126/science.1217576, 2012.
- Yu, R. C., Wang, B., and Zhou, T.: Climate effects of the deep continental stratus clouds generated by the Tibetan Plateau, *J. Climate*, 17, 2702–2713, 2004.
- 10 Yuan, T. and Oreopoulos, L.: On the global character of overlap between low and high clouds, *Geophys. Res. Lett.*, 40, 5320–5326, doi:10.1002/grl.50871, 2013.
- Zhang, M. H., Lin, W. Y., Klein, S. A., Bacmeister, J. T., Bony, S., Cederwall, R. T., Del Genio, A. D., Hack, J. J., Loeb, N. G., Lohmann, U., Minnis, P., Musat, I., Pincus, R., Stier, P., Suarez, M. J., Webb, M. J., Wu, J. B., Xie, S. C., Yao, M. S., and Zhang, J. H.: Comparing clouds and their seasonal variations in 10 atmospheric general circulation models with satellite measurements, *J. Geophys. Res.*, 110, D15S02, doi:10.1029/2004JD005021, 2005.
- 15

Title Page	Abstract	Introduction
Conclusions	References	
Tables	Figures	
◀	▶	
◀	▶	
Back	Close	
Full Screen / Esc		
Printer-friendly Version		
Interactive Discussion		



Distributions and overlap of various cloud types

J. Li et al.

Table 1. Comparison of Global cloud type occurrence frequency averages over land and ocean by using four different datasets. CloudSat (Radar-Lidar cloud classification): 2B-CLDCLASS-Lidar product (January 2007–December 2010); CloudSat (Radar-only cloud classification): 2B-CLDCLASS product (June 2006–June 2007). Surface: annual means of extended surface observer reports (Hahn and Warren, 1999); ISCCP: ISCCP Annual means from 1986–1993 (Rossow and Schiffer, 1999). Here, the statistical results of the latter three datasets all are from the study of Sassen and Wang (2008).

Type	CloudSat (Radar-Lidar) ^a		CloudSat (Radar- only)		Surface		ISCCP	
	Land	Ocean	Land	Ocean	Land	Ocean	Land	Ocean
High	23.3 (29.4)	25.2 (29.6)	9.6	10.9	23.1	14.0	19.3	15.6
As	13.2 (14.3)	10.3 (10.2)	12.7	12.0	4.8	6.5	8.7	9.7
Ac	12.3 (13.1)	9.5 (11.2)	6.8	6.7	17.2	17.1	8.6	10.2
St + Sc	16.7 (11.5)	31.3 (35.9)	13.5	22.5	18.9	39.4	10.7	18.3
Cu	9.0 (5.4)	12.5 (12.8)	1.7	1.7	4.2	9.8	7.7	12.7
Ns	5.5 (5.6)	5.7 (5.7)	8.6	8.3	6.3	7.9	3.2	3.0
Deep	1.2 (1.1)	1.1 (1.2)	1.8	1.9	3.2	5.3	2.5	2.4

^a The results from CloudSat (Radar-Lidar) are reported separately for day- and night-time. The values in parentheses indicate the cloud fractions of different cloud types during nighttime.

- [Title Page](#)
- [Abstract](#) | [Introduction](#)
- [Conclusions](#) | [References](#)
- [Tables](#) | [Figures](#)
- [◀](#) | [▶](#)
- [◀](#) | [▶](#)
- [Back](#) | [Close](#)
- [Full Screen / Esc](#)
- [Printer-friendly Version](#)
- [Interactive Discussion](#)



Distributions and overlap of various cloud types

J. Li et al.

[Title Page](#)

[Abstract](#)

[Introduction](#)

[Conclusions](#)

[References](#)

[Tables](#)

[Figures](#)

[|◀](#)

[▶|](#)

[◀](#)

[▶|](#)

[Back](#)

[Close](#)

[Full Screen / Esc](#)

[Printer-friendly Version](#)

[Interactive Discussion](#)



Table 2. Globally averaged overlapping percentages of different cloud types over land and ocean during daytime.

	SL ^a	ML ^b	High	As	Ac	St/Sc	Cu	Ns	Deep	surface
High	8.8	14.5	3.7	2.5	4.3	3.2	2.8	1.0	0.4	Land
	8.8	16.4	4.1	2.2	3.5	5.2	3.5	1.2	0.3	Ocean
As	6.5	6.7	—	0.9	1.0	2.0	1.1	0.4	—	Land
	4.2	6.1	—	0.5	0.9	2.5	1.0	0.3	—	Ocean
Ac	5.3	7.0	—	0.01	1.1	0.9	1.1	0.04	—	Land
	3.1	6.4	—	0.01	0.8	1.5	1.0	0.08	—	Ocean
St/Sc	10.5	6.2	—	—	—	0.3	0.5	—	—	Land
	21.9	9.4	—	—	—	0.4	0.7	—	—	Ocean
Cu	3.9	5.1	—	—	—	0.1	0.3	—	—	Land
	6.6	5.9	—	—	—	0.2	0.3	—	—	Ocean
Ns	4.0	1.5	—	—	—	0.02	0.09	—	—	Land
	4.1	1.6	—	—	—	0.02	0.05	—	—	Ocean
Deep	0.8	0.4	—	—	—	—	—	—	—	Land
	0.8	0.3	—	—	—	—	—	—	—	Ocean

^a The SL represents the single-layered cloud.

^b The ML represents the multi-layered cloud. And, those boldfaced values indicated the overlapping percentages of different cloud types over ocean.

Distributions and overlap of various cloud types

J. Li et al.

[Title Page](#)

[Abstract](#)

[Introduction](#)

[Conclusions](#)

[References](#)

[Tables](#)

[Figures](#)

[|◀](#)

[▶|](#)

[◀](#)

[▶|](#)

[Back](#)

[Close](#)

[Full Screen / Esc](#)

[Printer-friendly Version](#)

[Interactive Discussion](#)



Table 3. Globally averaged overlapping percentages for different cloud types over land and ocean during nighttime.

	SL ^a	ML ^b	High	As	Ac	St/Sc	Cu	Ns	Deep	surface
High	12.0	17.4	5.5	3.2	6.6	2.6	1.8	1.3	0.3	Land
	8.8	20.8	4.7	2.3	5.0	7.6	4.4	1.3	0.3	Ocean
As	6.9	7.4	—	1.0	1.1	1.9	0.9	0.4	—	Land
	3.9	6.3	—	0.4	0.9	2.6	1.0	0.3	—	Ocean
Ac	4.6	8.5	—	0.01	1.2	0.7	0.6	0.05	—	Land
	3.1	8.1	—	0.01	1.0	1.9	1.2	0.08	—	Ocean
St/Sc	6.4	5.1	—	—	—	0.2	0.3	—	—	Land
	23.8	12.1	—	—	—	0.4	0.8	—	—	Ocean
Cu	2.0	3.4	—	—	—	0.1	0.2	—	—	Land
	5.9	6.9	—	—	—	0.2	0.4	—	—	Ocean
Ns	3.9	1.7	—	—	—	—	0.08	—	—	Land
	4.0	1.7	—	—	—	—	0.05	—	—	Ocean
Deep	0.8	0.3	—	—	—	—	—	—	—	Land
	0.9	0.3	—	—	—	—	—	—	—	Ocean

^a The SL represents the single-layered cloud.

^b The ML represents the multi-layered cloud. And, those boldfaced values indicated the overlapping percentages of different cloud types over ocean.

Distributions and overlap of various cloud types

J. Li et al.

[Title Page](#)

[Abstract](#)

[Introduction](#)

[Conclusions](#)

[References](#)

[Tables](#)

[Figures](#)

[|◀](#)

[▶|](#)

[◀](#)

[▶](#)

[Back](#)

[Close](#)

[Full Screen / Esc](#)

[Printer-friendly Version](#)

[Interactive Discussion](#)



Table 4. Cloud fractions of different multilayered cloud types based on different overlap assumptions and observations during daytime. Here, C_{overlap} and $C_1 \cdot C_2$ are the overlap cloud fraction from observations and overlap assumptions. “ a ” presents the overlap parameter.

Cloud type	C_{max}	C_{random}	C_{real}	$C_1 \cdot C_2$	C_{overlap}	RD ^a	Diff. ^b	a
High + As	24.7 (26.3)	33.8 (33.2)	34.0 (33.3)	2.7 (2.2)	2.5 (2.2)	-0.4 % (-0.0 %)	3.8 % (-2.2 %)	-0.02 (0.01)
High + Ac	23.5 (25.2)	32.3 (32.2)	31.4 (31.1)	3.4 (2.4)	4.3 (3.5)	3.0 % (3.6 %)	-28.7 % (-32.8 %)	0.10 (0.17)
High + St/Sc	26.2 (37.2)	36.2 (49.5)	36.9 (51.3)	3.8 (7.0)	3.2 (5.2)	-1.5 % (-3.5 %)	19.0 % (35.9 %)	-0.05 (-0.15)
High + Cu	23.3 (25.2)	29.9 (34.2)	29.6 (34.2)	2.5 (3.5)	2.8 (3.5)	0.9 % (-0.1 %)	-8.9 % (3.2 %)	0.05 (0.0)
High + Ns	23.4 (25.8)	27.8 (29.8)	27.8 (29.6)	1.1 (1.1)	1.0 (1.2)	-0.01 % (0.6 %)	-4.2 % (-20.3 %)	0.06 (0.12)
High + Deep	23.3 (25.2)	24.1 (25.9)	24.2 (25.9)	0.4 (0.4)	0.3 (0.3)	-0.03 % (-0.1 %)	29.6 % (21.8 %)	-0.05 (-0.05)
As + St/Sc	17.4 (31.3)	27.3 (37.9)	27.9 (39.2)	2.6 (3.8)	2.0 (2.5)	-2.1 % (-3.2 %)	81.5 % (182 %)	-0.06 (-0.22)
As + Cu	15.2 (16.3)	21.1 (21.8)	21.1 (21.9)	1.1 (1.1)	1.1 (1.0)	-0.1 % (-0.5 %)	0.6 % (25.1 %)	0 (-0.02)
Ac + St/Sc	18.8 (31.3)	27.0 (37.8)	28.1 (39.3)	2.0 (3.0)	0.9 (1.5)	-3.4 % (-3.8 %)	116 % (98 %)	-0.12 (-0.24)
Ac + Cu	12.5 (13.5)	20.0 (20.8)	20.2 (21.0)	1.3 (1.2)	1.1 (1.0)	-0.4 % (-0.5 %)	4 % (11.6 %)	-0.01 (-0.02)

^a Calculated from $(C_{\text{random}} - C_{\text{real}})/C_{\text{real}}$.

^b Calculated from $(C_1 \cdot C_2 - C_{\text{overlap}})/C_{\text{overlap}}$. And, those boldfaced values in the brackets indicated the overlapping percentages of different cloud types over ocean surface.

Distributions and overlap of various cloud types

J. Li et al.

[Title Page](#)[Abstract](#)[Introduction](#)[Conclusions](#)[References](#)[Tables](#)[Figures](#)[|◀](#)[▶|](#)[◀](#)[▶](#)[Back](#)[Close](#)[Full Screen / Esc](#)[Printer-friendly Version](#)[Interactive Discussion](#)

Table 5. Cloud fractions of different multilayered cloud types based on different overlap assumptions and observations during nighttime. Here, C_{overlap} and $C_1 \cdot C_2$ are the overlap cloud fraction from observations and overlap assumptions. “ a ” presents the overlap parameter.

Cloud type	C_{max}	C_{random}	C_{real}	$C_1 \cdot C_2$	C_{overlap}	RD ^a	Diff. ^b	a
High + As	31.2 (30.5)	40.0 (37.2)	40.4 (37.5)	3.7 (2.6)	3.2 (2.3)	-0.9 % (-0.6 %)	12.8 % (7.4 %)	-0.06 (-0.04)
High + Ac	29.4 (29.6)	37.6 (37.2)	36.0 (35.8)	4.9 (3.6)	6.6 (5.0)	4.3 % (4.1 %)	-34.7 % (-32.4 %)	0.20 (0.19)
High + St/Sc	30.7 (43.5)	38.0 (56.1)	38.3 (58.0)	2.9 (9.4)	2.6 (7.6)	-0.8 % (-3.1 %)	11.5 % (24.9 %)	-0.02 (-0.15)
High + Cu	29.4 (29.6)	33.1 (38.2)	32.9 (38.0)	1.7 (4.2)	1.8 (4.4)	0.4 % (0.3 %)	-6.4 % (0.2 %)	0.07 (0.02)
High + Ns	29.5 (30.1)	33.6 (34.1)	33.7 (34.0)	1.3 (1.2)	1.3 (1.3)	-0.2 % (0.3 %)	3.1 % (-14.8 %)	0.02 (0.12)
High + Deep	29.4 (29.6)	30.0 (30.3)	30.2 (30.5)	0.5 (0.5)	0.3 (0.3)	-0.3 % (-0.3 %)	63.0 % (49.3 %)	-0.19 (-0.14)
As + St/Sc	14.7 (35.9)	23.7 (42.1)	23.9 (43.5)	2.1 (4.0)	1.9 (2.6)	-0.8 % (-3.2 %)	33.9 % (164 %)	-0.02 (-0.28)
As + Cu	14.3 (16.5)	18.9 (22.0)	18.8 (22.0)	0.8 (1.1)	0.9 (1.0)	0.9 % (-0.4 %)	-20.0 % (18.9 %)	0.03 (-0.02)
Ac + St/Sc	17.5 (36.0)	23.4 (43.2)	23.9 (45.2)	1.2 (3.9)	0.7 (1.9)	-1.9 % (-4.4 %)	68.3 % (121 %)	-0.08 (-0.3)
Ac + Cu	13.4 (13.8)	17.8 (22.5)	17.9 (22.7)	0.7 (1.5)	0.6 (1.2)	-0.3 % (-0.9 %)	6.4 % (17.3 %)	-0.02 (-0.03)

^a Calculated from $(C_{\text{random}} - C_{\text{real}})/C_{\text{real}}$.^b Calculated from $(C_1 \cdot C_2 - C_{\text{overlap}})/C_{\text{overlap}}$. And, those boldfaced values in the brackets indicated the overlapping percentages of different cloud types over ocean surface.

Distributions and overlap of various cloud types

J. Li et al.

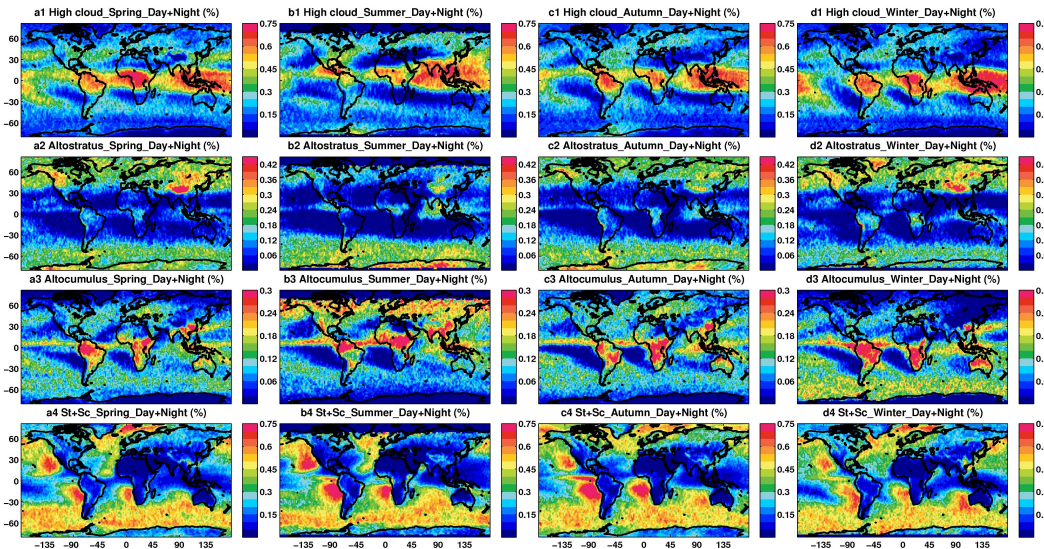


Fig. 1. The seasonal variations of mean day plus night frequencies for different cloud types averaged over $2^\circ \times 2^\circ$ grid boxes based on the 2B-CLDCLASS-Lidar product.

[Title Page](#)

[Abstract](#)

[Introduction](#)

[Conclusions](#)

[References](#)

[Tables](#)

[Figures](#)

◀

▶

[Back](#)

[Close](#)

[Full Screen / Esc](#)

[Printer-friendly Version](#)

[Interactive Discussion](#)

Distributions and overlap of various cloud types

J. Li et al.

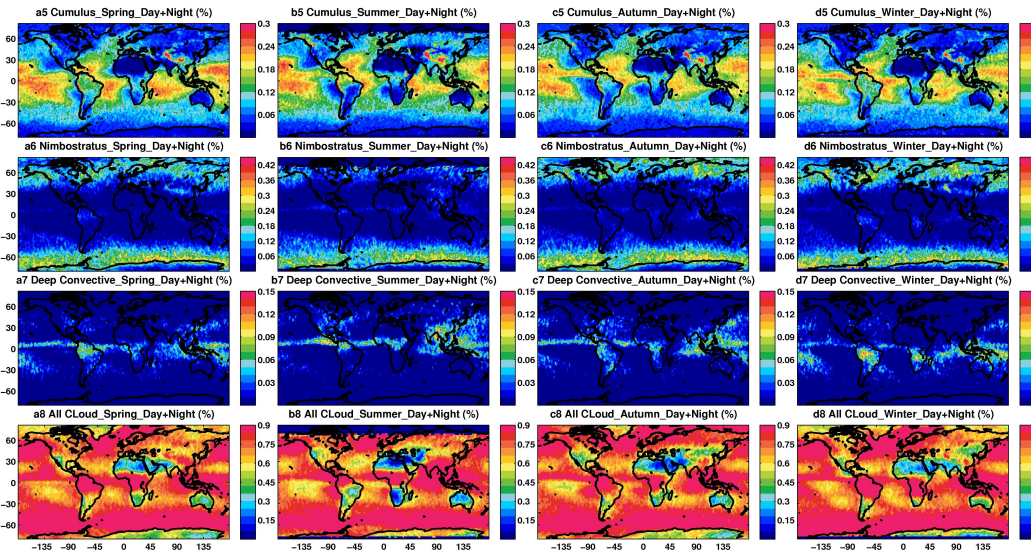


Fig. 1. The seasonal variations of mean day plus night frequencies for different cloud types averaged over $2^\circ \times 2^\circ$ grid boxes based on the 2B-CLDCLASS-Lidar product.

[Title Page](#)

[Abstract](#)

[Introduction](#)

[Conclusions](#)

[References](#)

[Tables](#)

[Figures](#)

◀

▶

◀

▶

[Back](#)

[Close](#)

[Full Screen / Esc](#)

[Printer-friendly Version](#)

[Interactive Discussion](#)



Distributions and overlap of various cloud types

J. Li et al.

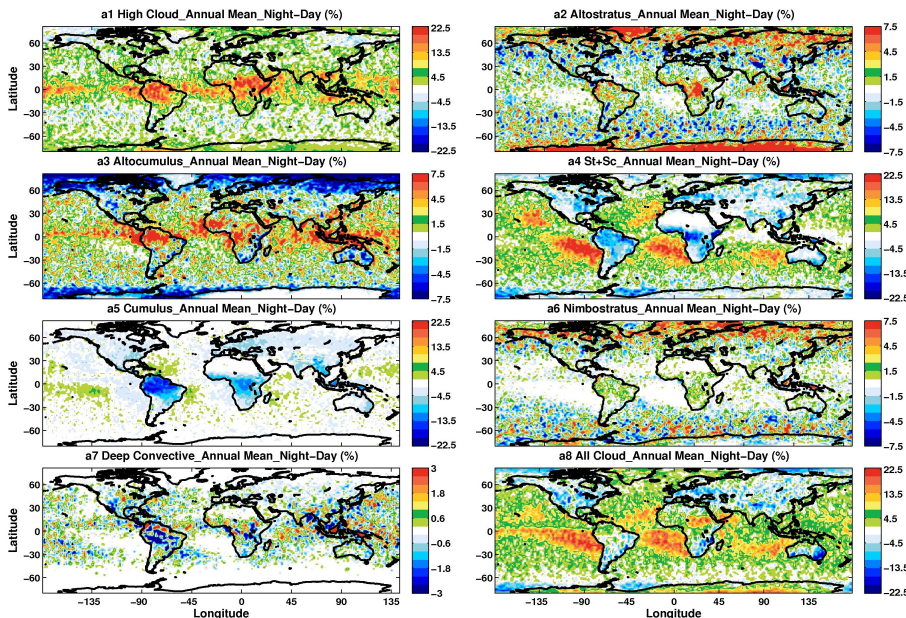


Fig. 2. The global distributions of annually averaged night minus day frequencies for different cloud types averaged over $2^\circ \times 2^\circ$ grid boxes based on the 2B-CLDCLASS-Lidar product.

[Title Page](#)

[Abstract](#)

[Introduction](#)

[Conclusions](#)

[References](#)

[Tables](#)

[Figures](#)

[|◀](#)

[▶|](#)

[◀](#)

[▶|](#)

[Back](#) [Close](#)

[Full Screen / Esc](#)

[Printer-friendly Version](#)

[Interactive Discussion](#)

Distributions and overlap of various cloud types

J. Li et al.

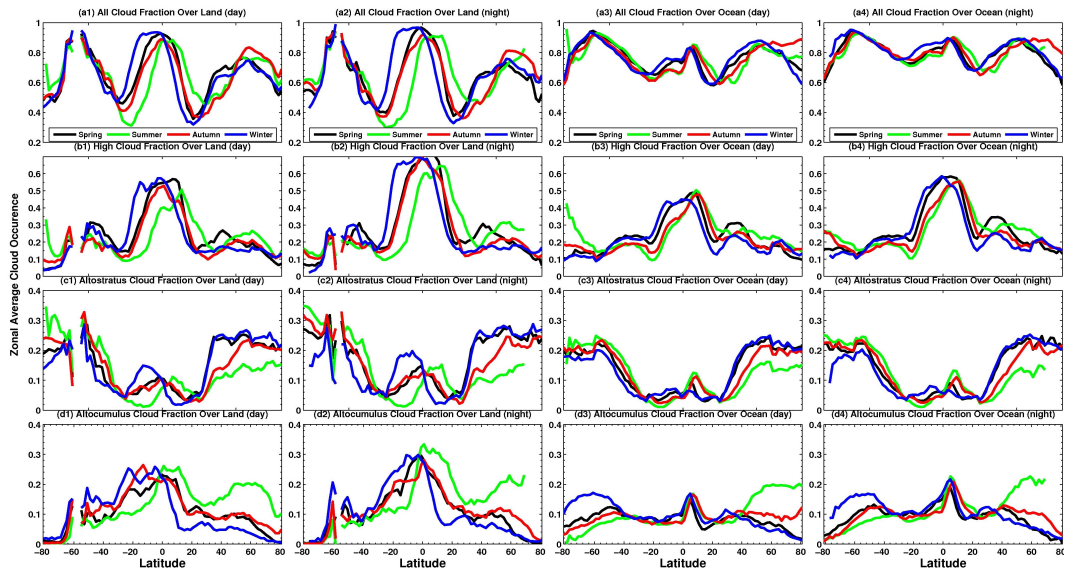


Fig. 3. The seasonal variations of zonal distributions for different cloud types over land and ocean during day- and night-time, respectively.

- [Title Page](#)
- [Abstract](#) [Introduction](#)
- [Conclusions](#) [References](#)
- [Tables](#) [Figures](#)
- [◀](#) [▶](#)
- [◀](#) [▶](#)
- [Back](#) [Close](#)
- [Full Screen / Esc](#)
- [Printer-friendly Version](#)
- [Interactive Discussion](#)

Distributions and
overlap of various
cloud types

J. Li et al.

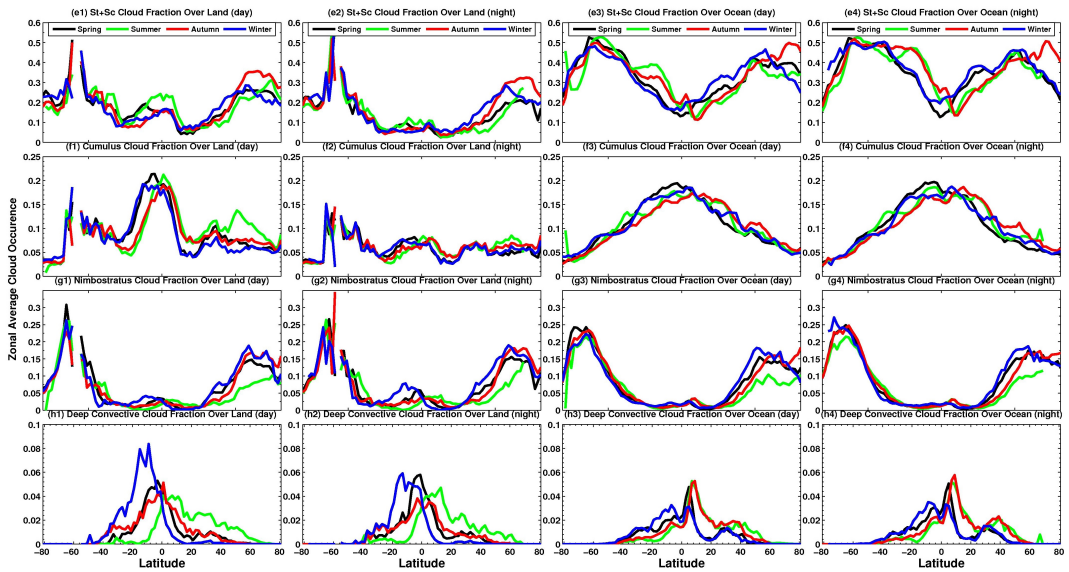


Fig. 3. The seasonal variations of zonal distributions for different cloud types over land and ocean during day- and night-time, respectively.

Distributions and overlap of various cloud types

J. Li et al.

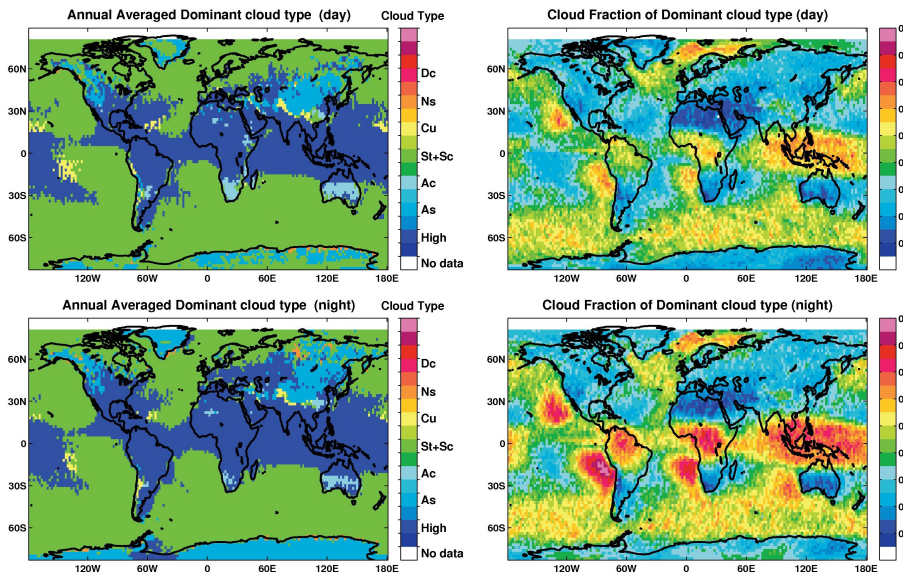


Fig. 4. The global distributions of the most frequent cloud type and the corresponding cloud fractions during day- and night-time.

Distributions and overlap of various cloud types

J. Li et al.

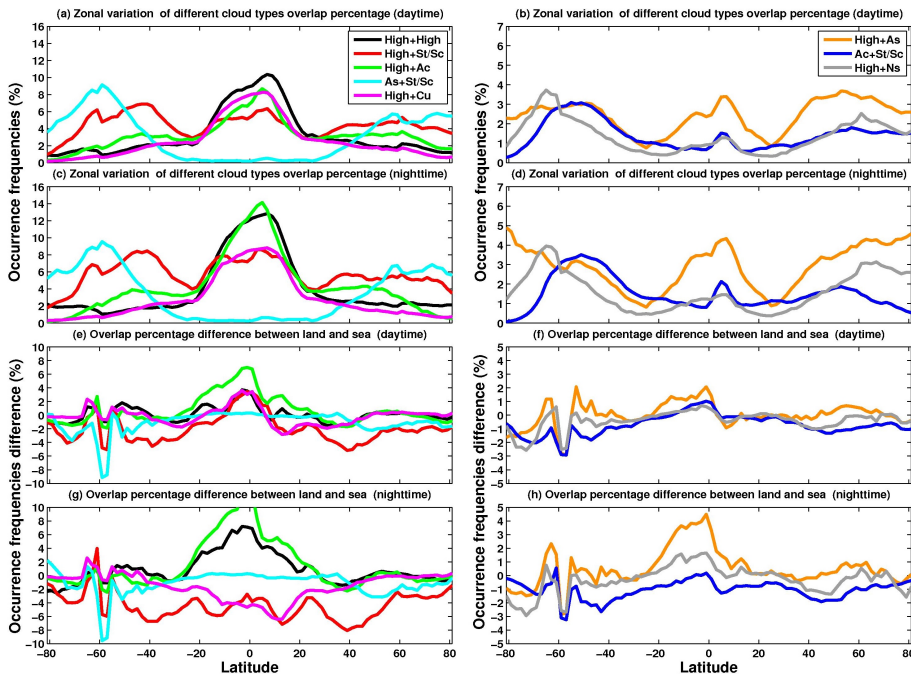


Fig. 5. (a–d): zonal distributions of annual most frequently occurring multilayered cloud types during day- and nighttime. **(e–h):** the zonal distribution differences of annual most frequently occurring multilayered cloud types between land and ocean during day- and nighttime.

Title Page

Abstract

Introduction

Conclusions

References

Tables

Figures



Back

Close

Full Screen / Esc

Printer-friendly Version

Interactive Discussion



Distributions and overlap of various cloud types

J. Li et al.

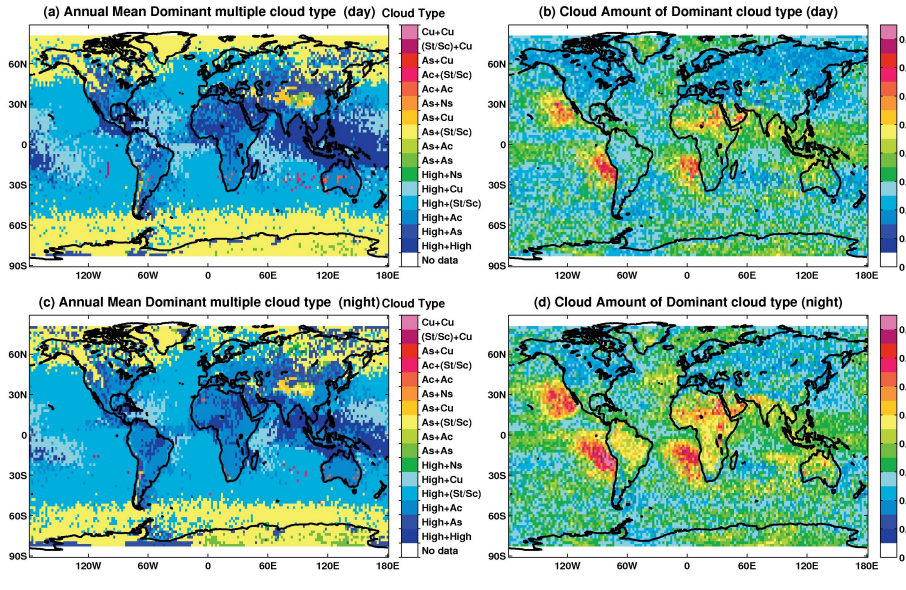


Fig. 6. The global distributions of the annual most frequently occurring multilayered cloud types and the corresponding cloud amounts during day- and night-time.

Distributions and overlap of various cloud types

J. Li et al.

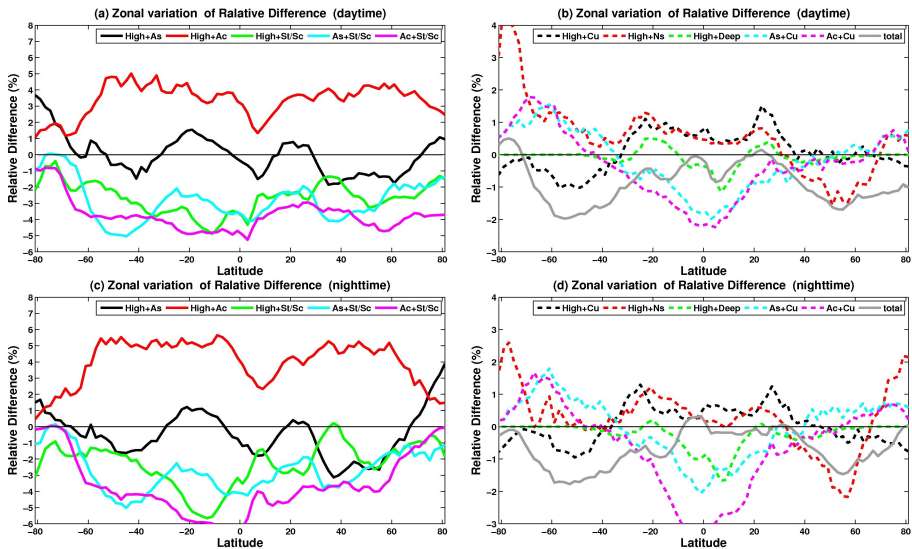


Fig. 7. The zonal distributions of relative difference in cloud fraction between random overlap and real overlap for main ten multilayered cloud types and the cumulative relative difference of all multilayered cloud types during day- and night-time.

Title Page

Abstract

Introduction

Conclusions

References

Tables

Figures

◀

▶

◀

▶

Back

Close

Full Screen / Esc

Printer-friendly Version

Interactive Discussion

Distributions and overlap of various cloud types

J. Li et al.

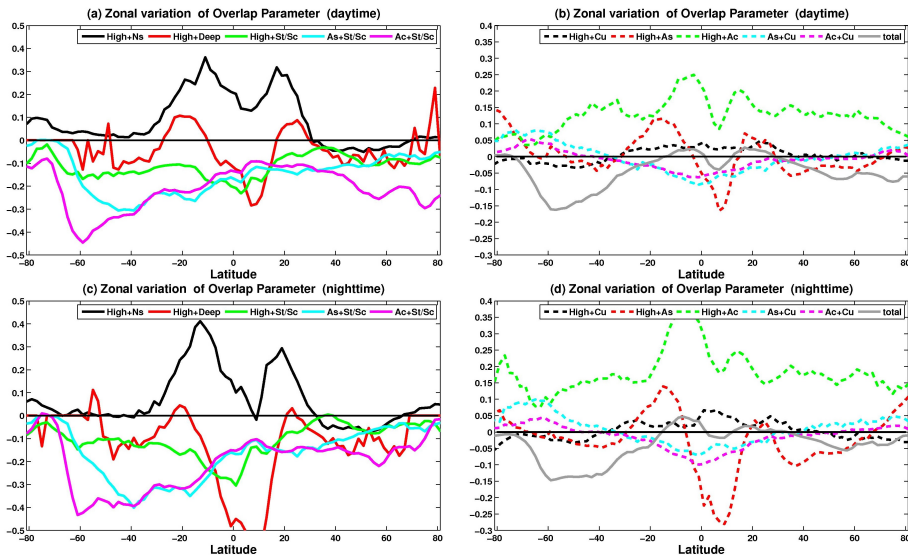


Fig. 8. The zonal distributions of overlap parameter of cloud fraction for main ten multilayered cloud types and the cumulative overlap parameter of all multilayered cloud types during day- and night-time.

Distributions and overlap of various cloud types

J. Li et al.

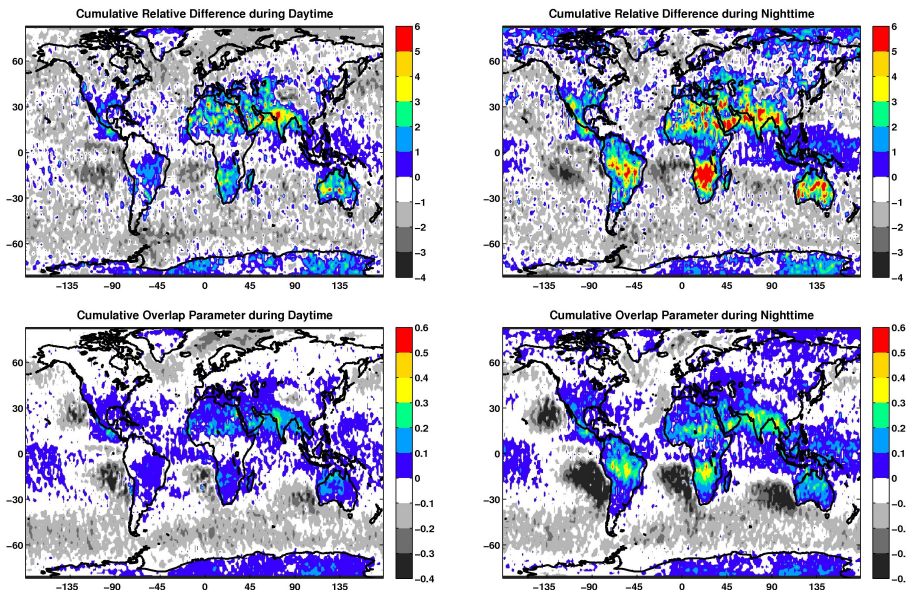


Fig. 9. The global distributions of the cumulative relative difference and the cumulative overlap parameter of all multilayered cloud types during day- and night-time.

- [Title Page](#)
- [Abstract](#) [Introduction](#)
- [Conclusions](#) [References](#)
- [Tables](#) [Figures](#)
- [◀](#) [▶](#)
- [◀](#) [▶](#)
- [Back](#) [Close](#)
- [Full Screen / Esc](#)
- [Printer-friendly Version](#)
- [Interactive Discussion](#)